MODELLING AND EXPERIMENTAL SETUP OF A CABLE DRIVEN SYSTEM

A Thesis Submitted to
the Graduate School of Engineering and Sciences of
İzmir Institute of Technology
in Partial Fulfillment of the Requirements for the Degree of

MASTER OF SCIENCE

in Mechanical Engineering

by
Talha ERAZ

July 2016
İZMİR

We approve the thesis of **Talha ERAZ**

Examining Committee Members:

Assist. Prof. Dr. Gökhan KİPER
Department of Mechanical Engineering, İzmir Institute of Technology

Assist. Prof. Dr. Mehmet İsmet Can DEDE
Department of Mechanical Engineering, İzmir Institute of Technology

Assist. Prof. Dr. Fatih Cemal CAN
Department of Mechatronics Engineering, İzmir Katip Çelebi University

Assist. Prof. Dr. Erkin GEZGİN
Department of Mechatronics Engineering, İzmir Katip Çelebi University

Assist. Prof. Dr. Özgür KİLİT
Department of Industrial Design, Yaşar University

14 July 2016

Assist. Prof. Dr. Gökhan KİPER
Supervisor
Department of Mechanical Engineering
İzmir Institute of Technology

Assist. Prof. Dr. M. İ. Can DEDE
Co-Supervisor
Department of Mechanical Engineering
İzmir Institute of Technology

Prof. Dr. Metin TANOĞLU
Head of the Department of
Mechanical Engineering

Prof. Dr. Bilge KARAÇALI
Dean of the Graduate School of
Engineering and Sciences

ACKNOWLEDGMENTS

I would like to express my gratitude to my supervisor Assist. Prof. Dr. Gökhan KİPER for all the guidance he has offered, all inspiration he gave and especially all patience he has shown, and to my co-supervisor Assist. Prof. Dr. Mehmet İsmet Can DEDE for all he taught and the courage he gave. I also would like to thank Mr. Jascha Norman PARIS, my supervisor during my studies in RWTH Aachen, Univ.-Prof. Dr.-Ing. Burkhard CORVES and Prof. Dr.-Ing. Mathias HÜSİNG, academic instructors in Department of Mechanism Theory and Dynamics of Machines of RWTH Aachen University.

ABSTRACT

MODELLING AND EXPERIMENTAL SETUP OF A CABLE DRIVEN SYSTEM

This study is about a single degree of freedom mechanism to be used for human arm rehabilitation purposes and actuated with cable-drive. The purpose of the design is to support rehabilitation motions with a single degree of freedom (dof) mechanism. Design criteria is set based on research and meetings with medical doctors. The desired design is an exoskeleton type system to support human arm on each moving part of it.

The first designed four- bar mechanism had actuation problems. Torque requirement was unacceptably high near the singularity of the designed four-bar mechanism. This problem is later overcome by an extra dyad of two additional links. However, the extra dyad solution caused problems of back-drivability near the singularity of new dyad.

In order to achieve a back-drivable four-bar mechanism that has a smooth actuation requirement through the motion, a novel cable actuation system is designed. Cable is attached to system on coupler link and the attachment point on the coupler is designed to achieve a straight path for the efficiency of the cable drive. However, a single straight line throughout the motion is not achievable. Therefore, path is divided into subsections of straight line paths. Intermediate pulleys are placed for cable to follow straight line sections. The cable is designed as closed loop. A prototype of the system is built and presented in last chapter.

ÖZET

KABLO TAHRİKLİ BİR SİSTEMİN MODELLENMESİ VE DENEY DÜZENEĞİNİN KURULMASI

Bu çalışma, kablo tahrikli, tek serbestlik dereceli, insan kolu için tasarlanmış bir fizik tedavi mekanizması ile ilgilidir. Tasarlanan ilk mekanizmanın amacı, tek serbestlik dereceli bir sistem ile omuz ve kol sakatlıklarının tedavisinde yapılan fizik tedavi hareketlerinin desteklenmesidir. Çalışmanın tasarım kriterleri, yapılan araştırmalara ve Dokuz Eylül Tıp Fakültesi'nden öğretim üyeleri ile yapılan görüşmelere dayanmaktadır. Tasarımın amacı, insan kolunu fizik tedavi egzersizleri sırasında hareketli her kısımdan ayrı ayrı desteklemektir.

Tasarımı yapılan ilk dört çubuk mekanizmasının eyleme sorunu tespit edilmiştir. Mekanizmanın tekil pozisyonlarına yakın konumlarda eyleyici torku gereksinimi Kabul edilemez düzeyde yüksek çıkmıştır. Bu problem, sonradan 2 uzuvlu bir ekleme ile aşılmıştır. Ancak bu çözümde de, eklenen uzuvların tekil konumlarında geri sürülebilirlik sağlanamamıştır.

Geri sürülebilir, dengeli eyleyici gereksinimi olan bir system için özgün bir kablo tahrik sistemi tasarlanmıştır. Tahrik amaçlı olarak bir kablo, sisteme biyel uzvundan bağlanmış, bağlanacağı nokta da kablo tahrik sisteminin verimliliği açısından düz bir çizgi üzerinde hareket eden bir konumda seçilmiştir. Ancak, mekanizmanın hareketinin başından sonuna kadar düz bir çizgi üzerinde hareket eden tek bir nokta bulunamamıştır. Bunun yerine, parametrik olarak tanımlanan bir noktanın, birkaç düz çizgi çizerek hareket etmesi amaçlanmış, sonuç olarak da hareket birkaç düz çizgiye bölünmüştür. Motor makarası dışında pasif makaralar eklenmiş, kablonun seçilen bağlantı noktasının takip ettiği düz çizgilerin üzerinde kalması sağlanmış ve tahrik kablosu kapalı devre haline getirilmiştir. Sistemin deney düzeneği kurulmuş ve düzenek son bölümde aktarılmıştır.

TABLE OF CONTENTS

LIST OF FIGURES

Figure **Page**

CHAPTER 1

INTRODUCTION

Stroke is a worldwide serious health issue and major part of patient care solution is rehabilitation. Stroke is classified by means of damage in terms of pathology, impairment, limitations in activity and handicaps. Effect of stroke is determined by the size of stroke lesion. [1]

Rehabilitation of a stroke patient is a complicated process. The system introduced in this study focuses on motor rehabilitation of stroke patients. Motor rehabilitation involves a mixture of approaches [2]. Urgent procedures are applied within hours after stroke in clinic environment. After the first days following the stroke, impairments are restored within weeks and task-oriented practices are applied for months (Figure 1). Daily living activities are improved by task-specific rehabilitation for months after stroke.

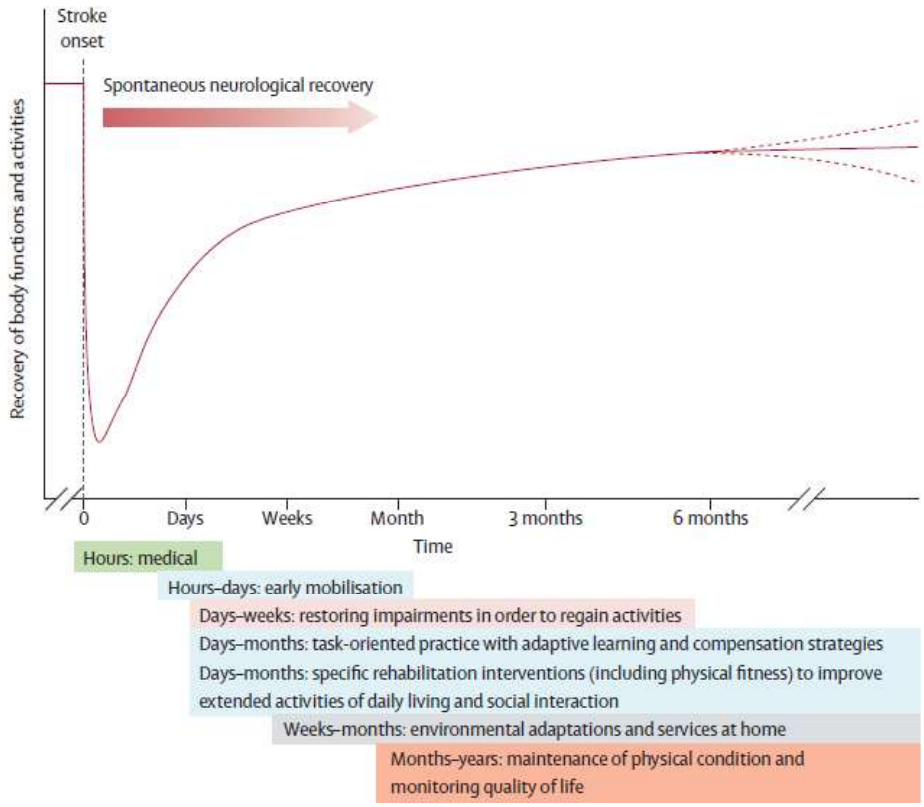

Figure 1. Stroke Rehabilitation Process [1]

Task-oriented training is aims to retrain functions of impaired parts by considering improvement of all related sub-systems in human body such as neural or musculoskeletal. Task-specific training focus on improving patient's ability to perform a specific task [2]. There are treatments enriched with robotic devices beside the traditional human-supported treatments. For task-oriented training, computer guided virtual reality exercises are commonly in use [3]. For task-specific rehabilitation, patients repeatedly perform a specific activity of daily life.

Medical doctors monitor the process for each patient in order to decide when the task-oriented or task-specific trainings start. Therefore the beginning and end of each different type of treatment period is mentioned as "days, weeks, months" instead of specific times. The purpose of the system designed in this thesis is task-specific training which may take two to four years.

Physical therapy and rehabilitation (PTR) has been a field of study of medical sciences for centuries and of robotics for decades. Before rehabilitation robots were introduced, the PTR therapists were responsible for helping patients to perform exercises and tracking the success of treatment process. Rehabilitation robotics aims to decrease the mentioned workloads of the therapists.

PTR patients may have limitations on mobility of parts of their body or the whole body. PTR process focus on improving mobility of a single joint or an extremity as a whole unit. Separate exercises are required for upper (arm) and lower (leg) extremities.

Rehabilitation robots are classified related to which section or extremity of the body they are built for. Another classification can be done related to interaction with the body. There are two main type of rehabilitation robots in that manner; end-effector type [4] and exoskeleton type [5]. End-effector type interacts with body through only one part and has a parallel, serial or hybrid kinematic chain that connect to base. Examples of this type are more common in early era of rehabilitation robotics [6, 7]. End-effector type robots are more adaptable and simpler by structure [8]. However end-effector type require extra equipment to support other moving parts of human body as treatment process suggests. Exoskeleton type, on the other hand, covers the body parts that form the extremity to be rehabilitated like an external skeleton and follows the practical

degree of freedom dof of that extremity. The only single dof upper limb rehabilitation system found in literature is by Xydas et al [9] which is an analysis study of straight line generating four-bar linkages. The point on the linkage that make straight line motion is designed to be attached to patient and therefore the system will work as end-effector type. This study introduce a four-bar mechanism which work as an exoskeleton. Links of mechanism are designed to be fixed on parts of arm and move together. Details are given in Planar Linkage Design Section.

1.1. Motivation

Report of the 1992 American Physical Therapy Association House of Delegates indicate several problems that physical therapists may face through their carrier [10]. Physical hazards include injuries and physical attacks from violent (receiving treatment for brain injury) patients. Besides chemical, physiological and radiation hazards, there is always a risk of infectious diseases as therapists need to be in contact with the patient. Though clinic regulations and treatment procedures aim to limit the risk of any kind up to a point, rehabilitation robotics improve working conditions of therapists further and help them to deal with more patients with same effort.

Success of a traditional rehabilitation process with a therapist may be tracked by having separate tests, imaging or observation. Rehabilitation robots, on the other hand, could track the response of patient and regulate the support accordingly in adaptive control [11]. The feedback based control supply real-time information on the reactions of patient during therapy [9]. This data is useful not only for tracking the treatment process but also for scientific purposes.

The patients need to perform most of their daily exercises at home with help of others which may be called usual care. A case study [12] on patients shows that robot assisted therapy is proven to outperform usual care within 36 weeks Patients are chosen to have had stroke 6 months prior to study, therefore all patients received usual care and robot-assisted therapy between 6 months and 15 months after stroke. 12 weeks of different treatments did not make a certain difference. However, robot-assisted therapy resulted in unarguably better results.

On the patient point of view, multi-dof rehabilitation robots are complex to use and hard to afford. The purpose of this study is to build a limited robot in terms of exercises it can do that is easy to use and affordable to build. The system is selected to support only the most common exercises for upper extremity rehabilitation.

1.2. Problem Definition

Main purpose of this study is to design a single dof mechanism to support certain therapy exercises for upper extremity (arm). A single dof mechanism may support limited number of motions. Therefore, exercises must be chosen as most common and mostly needed ones.

This study is based on a joint study with medical professors. A group of students, including author of this study, had visits to Dokuz Eylül University Hospital PTR clinic. The result of these meetings with medical doctors is explained in [13]. Group of patients that this study targets is chosen to be of age 30 to 70 at acute or subacute level of stroke. Task-specific robot-assisted exercises give the most outcome in the later stages of the rehabilitation [1], so the system to be designed in this study is expected to be used in the later stages of rehabilitation, where the spasm in the upper limb is already mostly resolved via medication and manual therapy. Some measurements are taken from patients in order to ensure the force requirements. The measurement method is explained in Figure 2. Arm is attached to a force meter at the elbow. Arm is pulled in abduction and vertical flexion directions as shown in Figure 2. Maximum force during the motion is noted. Measured force exceeded only up to 20% of the expected arm mass. Hence, the main aim of the rehabilitation mechanism is balancing the arm mass. However, the system should be able to actuate the motion in both directions in order to compensate force effects other than the weights of the arm parts, such as the spasm effects not yet resolved after the former rehabilitation treatments.

At the early stages of the mechanism supported rehabilitation, the patient's arm may be fully passive such that he/she cannot move the arm even a bit. At this stage, the mechanism works as a fully assistive device. As the rehabilitation continues, the patient starts to be able to move his/her arm and the mechanism works as a semi-assistive

device. When the mechanism is fully assistive, the actuation force requirements will be more than the semi-assistive case, so the actuation force requirements are determined accordingly. On the other hand, the system needs to be back-drivable during the semi-assistive period considering possible emergencies, therefore the mechanical advantage of the system throughout the motion is to be taken into account.

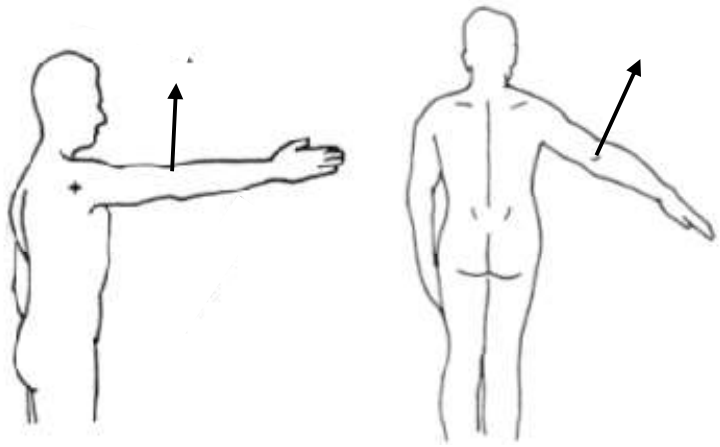

Figure 2. Schematic View of Measurements Taken [14]

Some important points noted in meetings with medical doctors is as follows. Supporting each part of arm in motion is essential in treatment process in order to decrease the load on joints and muscles. Exoskeleton type rehabilitation robots is designed for this purpose and end-effector type have additional independent supporting tools. End-effector type examples in the literature are mentioned in next part. They only ensure the position of hand as predefined task for patient. In order to ensure the arm to achieve the motion of exercise and it is supported on all parts, an exoskeleton that covers all parts to be supported should be part of synthesized kinematic chain.

Another important outcome of meetings with medical professors is that the target motions are decided. Motions to be supported are decided to be synergic planar motions which are exercises that include more than one joint and muscle group to be active. It is strongly suggested by medical doctors that synergic motions should be preferred instead of single motions in which a single joint is active. Besides, the hardest exercises to be supported by a PTR therapist are synergic motions.

The first motion is in vertical plane. Patients take their hand from a far front point to the back side of their head. The second motion is in an oblique plane that makes 60° with the vertical plane. Patients move their hand on a straight line from the front of their mouth to a short distance further and back in order to exercise for eating. Both motions are shown schematically in Figure 3. Point of view for both schemes is normal to planes of motions.

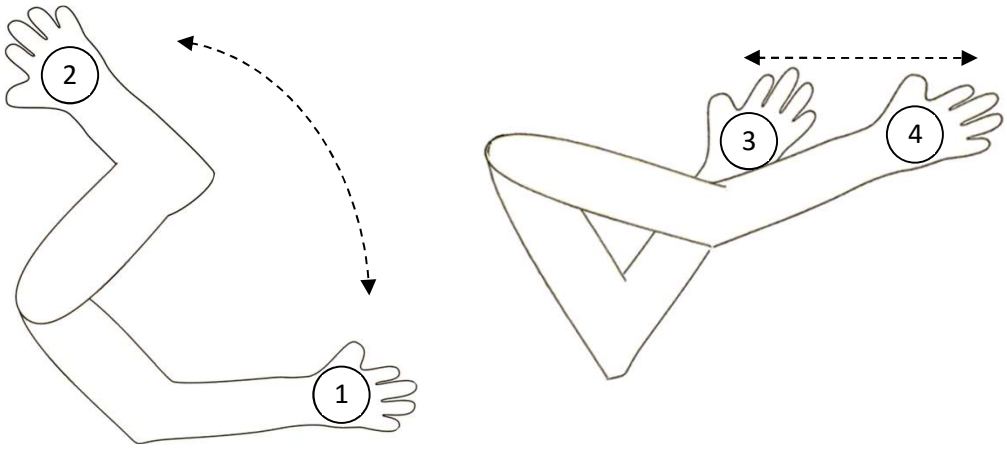

Figure 3. Schematic view of exercise in vertical plane (L) & in oblique plane (R)

Motions are defined such that the kinematic chain of arm takes the same planar shape in the final position of first motion (2) and the beginning of second motion (3). Two motions are in separate planes and the motion must stop at (2) in order to switch between planes of motion. Part of the problem is designing a reconfigurable frame such that the mechanism move to the other plane of motion without detaching patient's arm from the system although this reconfiguration will be used once to switch between exercises. This reconfigurable mechanism should also support the whole weight of mechanism, actuation instruments and arm. An additional momentary weight due to unexpected body motion of the patient should also be taken into account.

The rehabilitation mechanism to be designed in this study is to be a rather simple and relatively cheap system so that the treatment can be applied at the patient's house for up to a couple of years until the end of the therapy. It is a hard task to design a system suitable for all ranges of ages and dimensions of people, therefore, a patient-specific design methodology is preferred. The design is performed for specific height

and mass values in this thesis, however the design procedure can be easily adapted for any height and mass of the patient.

The outline of the thesis is as follows: First, this chapter is finalized with a review on rehabilitation robotics. In Chapter 2 the first rehabilitation mechanism design with a planar four-bar mechanism is explained with detailed problem parameters, design methodology, resultant mechanism, analysis method and result of analysis and finally the reconfigurable support design. However, the first version of the design has some actuation problems to be overcame and hence some modifications are made. First part of Chapter 3 includes the extra dyad solution and analysis of it. In the second part, cable drive solution is introduced with a modified four-bar mechanism design, design parameters, optimization procedure and analysis results. Chapter 4 is about the prototype of the final design which is a combination of the cable actuated mechanism introduced in Chapter 3 and the reconfigurable support introduced in Chapter 2. Chapter 5 concludes the study.

1.3. Literature Review

This section briefly summarizes the required information gathered from literature during this study. Kinematics of human arm is investigated first and the kinematic chain to be worked on is disclosed at the end of the review. The existing solutions of rehabilitation robotics are investigated and several successful studies are summarized in last part.

1.3.1. Kinematics of Human Arm

Erkin Gezgin explained in his M.Sc. Thesis that shoulder can be modelled as a spherical parallel manipulator [15]. Also, the shoulder joint (Figure 4), where humerus is connected to scapula, is a ball and socket type joint that that has allowance to a wide range of motion. Although there are two spherical joints serially connected that have closely placed centers, shoulder is modelled as a single spherical manipulator which is a spherical joint by means of kinematics.

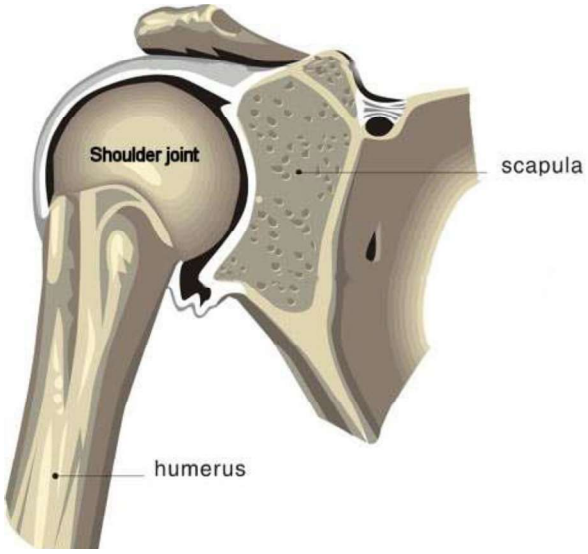

Figure 4. Structure of Shoulder Joint [15]

Elbow joint (Figure 5) is where humerus is connected to radius and ulna. The connection allows single dof rotation between humerus and other two bones (radius and ulna) combined. This joint also allows rotation of forearm and hand around radius. Twist motion of forearm that makes hand rotate around the axis of forearm is the rotational freedom in elbow joint. However, the latter will not be of use in this study as the designed system is planar.

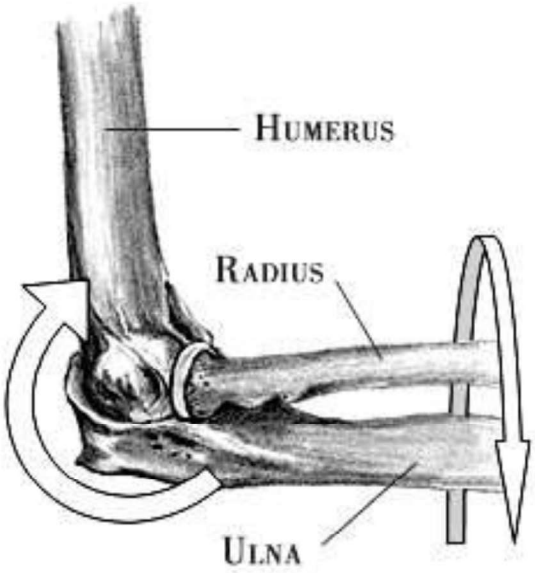

Figure 5. Elbow Joint [15]

1.3.2. Rehabilitation Robotics

Scientists in robotics introduced many solutions to aid rehabilitation of patients of many kinds. This section only covers the definition and comparison of different types and includes some examples of other studies. Rehabilitation robots are classified into two main groups as mentioned before: end-effector type and exoskeleton type.

End-effector type robots interact with patient only on one part of body which is usually chosen to be hand for arm rehabilitation robots. Sheng et al. [8] explain briefly that end-effector type also have two sub-types: table-top planar robots like MIT-MANUS [6] and multi-robots that work together to perform predefined motions with arm, like iPAM [16]. Multi-robots have the advantage of exercising one joint only, if needed. Table-top planar rehabilitation robots are rather simple but have risk of injuries when the rest of the arm is not supported by additional equipment. Sheng et al. (5) mention another end-effector type called the bilateral type. The bilateral type is simply two end-effector type robots attached to separate arms of patient. One of the arms is less impaired than the other, which guides the exercise, and more impaired arm follows the motion with aid of bilateral system.

Exoskeleton type robots enclose the impaired extremity such that all moving parts of the body are supported. Kinematic length of parts, joint type and freedom of joints must match that of the supported extremity in order to ensure all joint axes of body and exoskeleton match one by one. Though first examples of exoskeleton robots are made to increase strength of human body, most of exoskeleton robots in past decades are for rehabilitation purposes [17]. Gopura et. al. presented a review study on upper-limp exoskeleton robots which briefly mention human arm anatomy, evolution of arm exoskeleton robots and the study describes the criterion by which these robots are classified. As mentioned in [17], upper-limp exoskeleton robots are evaluated by the point of application, degree-of-freedom, kinematic structure, actuation or power transmission type, method of control and purpose. There are several successful studies in literature some of which are commercially available for use.

First model of ARMin was produced in early 2000s. This system is based on semi-exoskeleton model. Exoskeleton robot aids and traces motion of arm only on

forearm and hand. Kinematic chain that connects the support on forearm to base has 5 revolute joints in series. ARMin does not have support on upper arm (Figure 6). This model is now commercially available as Armeo brand name and has a variation of products.

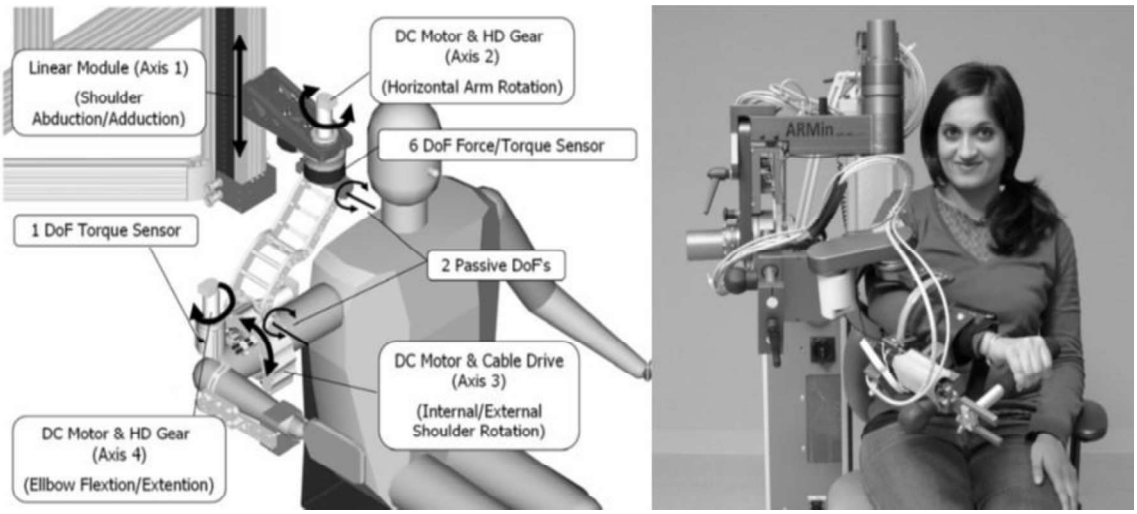

Figure 6. ARMin First Design [18] and ARMin III [19]

CAREX [20-26] is another multi-dof exoskeleton rehabilitation robot. The system first had an attachment on shoulder on which all actuators were attached. As shoulder joint is not a stable point on body during arm motion, placing actuating elements on shoulder itself makes it possible to design without having to consider the shoulder motion. The system has only 4 dof and 6 actuators due to single direction actuation handicap of cable drive. Cables (except Bowden cables) can only pull but not push. Extra cables may be needed not to lose on workspace or make use of all dof in one joint. At the beginning of this study, actuators were on shoulder and cables were parallel to the central axis of upper arm (Figure 7.a). Further optimizations brought more complicated cable attachment design. Another change in the design is that the actuators are moved to a fixed frame on top and the attachment on the shoulder is used as a pulley-holder for transmission of cables (Figure 7.b). This became a must after larger motors needed for the system.

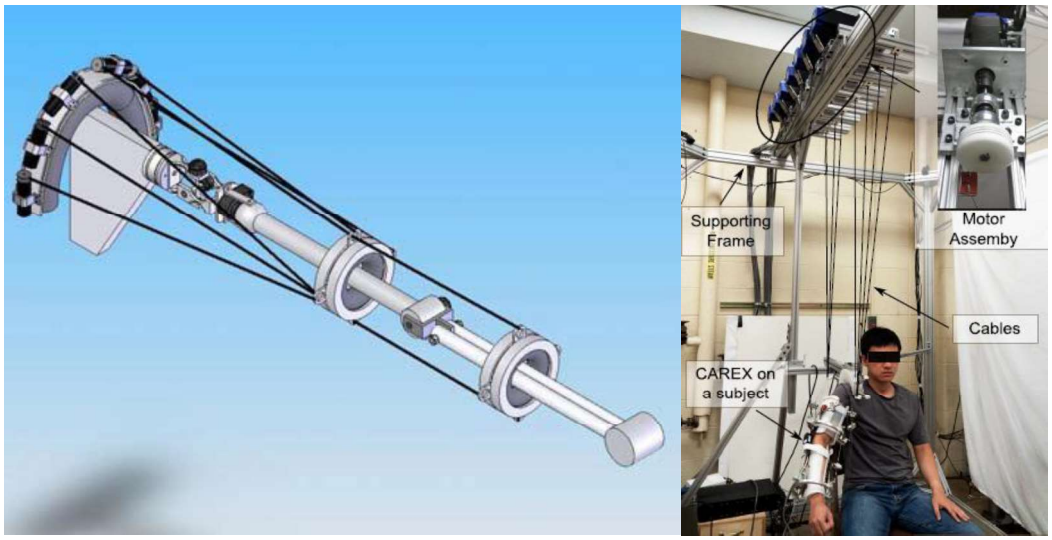

Figure 7. (a) CAREX First Design (left) (b) Final Design (right)

Another example of evolutionary exoskeleton rehabilitation robot design is MEDARM. The system [27] is first designed for planar motions of arm (Figure 8.a), including wrist. 4 cables are used to actuate 3 dof system similar to 4 dof CAREX is actuated with 6 cables. Later, system is evaluated to support 5 dof spatial motions of arm, excluding wrist, with 5 cables only. Though the system had 5 dof, supported motion is 4 dof, 3 axes rotations of shoulder and one rotation of elbow. Similar to CAREX, 4 dof motion is supported by exoskeleton but using 5 actuators and cables instead of 6.

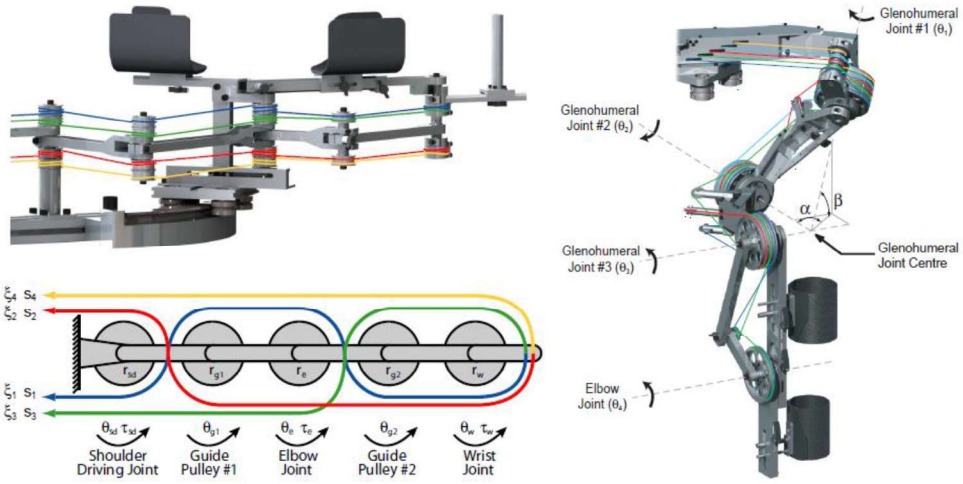

Figure 8. MEDARM (a) 3 dof Planar Design (b) 5 dof Spatial Design

Exoskeleton rehabilitation systems mentioned above are fixed to base and therefore cable drive is preferred to reduce moving weight. There are also wearable systems like ABLE [28-31]. This system is a 4 dof exoskeleton (Figure 9) actuated by compact cable transmissions. 2 actuators are placed inside the back module and 2 remaining are placed in the arm module (Figure 10). The 4 dof version of the system is reported to face some ergonomics problems [29]. This study is continued to develop a 7 dof version in which arm lengths are adjustable.

Figure 9. ABLE

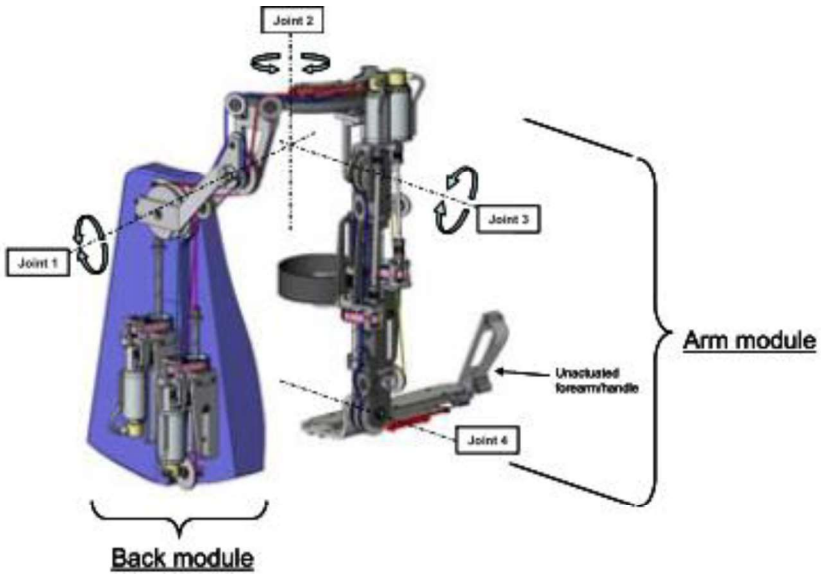

Figure 10. Actuator Mounting and Power Transmission of ABLE

Some other solutions for arm rehabilitation is rather simpler. Papadopoulos et al. [32] designed a four-bar that works together with a Genova mechanism. The system only supports upper arm and actuate shoulder joint for one axis rotation.

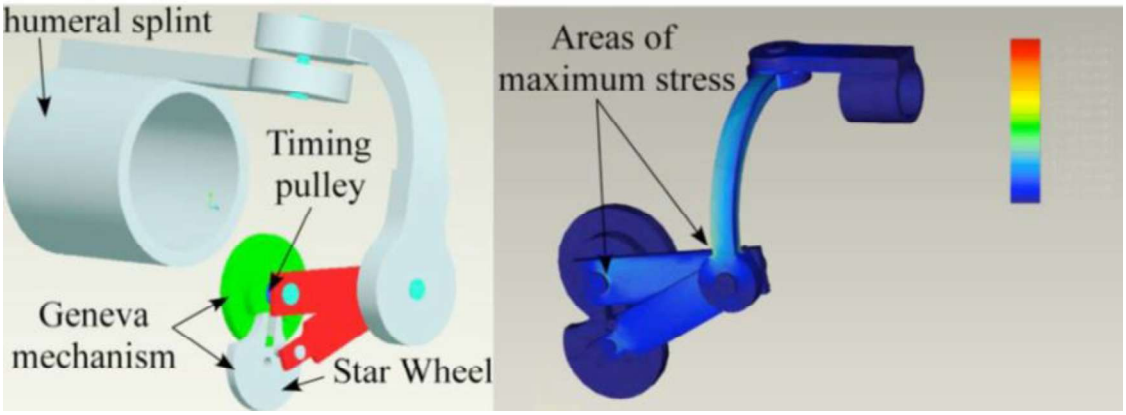

Figure 11. Shoulder Rehabilitation System with Geneva Mechanism [32]

Galiana et al. [33] designed a wearable soft system for shoulder motions and used cable transmission in actuation. Nunes et al. [14] designed a cable driven parallel manipulator for rehabilitation (). Moving platform of the system may be replaced with required attachments to fit different sections of human arm. Depending on the exercise, the attachment is replaced and 4 cables are attached to the new platform which will be rigidly attached to one or more part of the human arm. The review study of Gopura et al. [17] gives more examples and make comparisons of exoskeleton rehabilitation robots for upper limb.

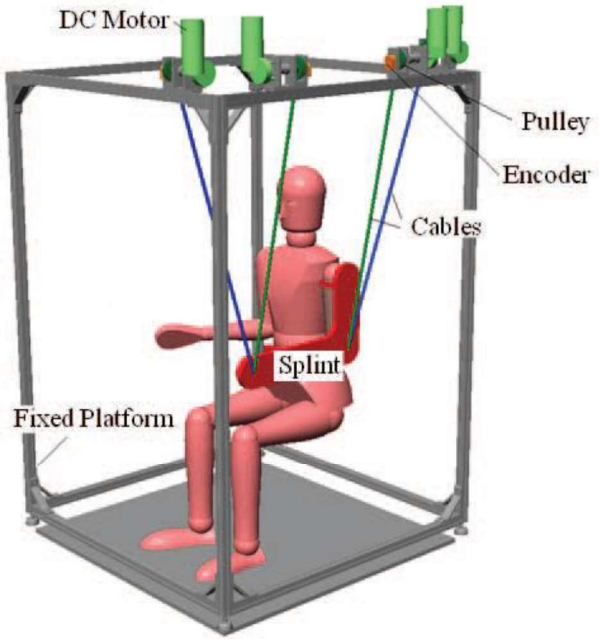

Figure 12. Arm Rehabilitation with a CDPM [14]

The literature contain many other studies similar to the ones mentioned. This study is, as explained in upcoming chapters, is rather a limited system by means of adaptability. A single dof mechanism is preferred instead of multi-dof for simplicity and cable actuation is used in a way that is not encountered in literature search which is the novel part of this study.

CHAPTER 2

KINEMATIC DESIGN

The arm motion problem in this study is modelled as planar three position motion synthesis. There are two exercise motions one of which ends at the planar position where the other one starts. Planar mechanism must move from one plane to another before the other motion begins. Therefore the system must have two sub-systems, a planar mechanism to support both planar motions and a mechanism or a joint to change the plane of motion of the planar mechanism.

2.1. Planar Linkage Design

2.1.1. Methodology

Human arm is a serial kinematic chain. The mechanism to be designed needs to support both upper arm and forearm during the motion. An end-effector type manipulator is not suitable for this purpose, so an exoskeleton type-mechanism is designed. At this point, the kinematics of the human arm is considered in order to obtain a fully supportive mechanism. Shoulder joint may be modelled as a ball-socket joint that allows rotations in all three axes which is a spherical kinematic pair. Elbow joint has two rotational axes. One of the rotation axes is perpendicular to upper arm and forearm central axes. The other rotation axis is along the forearm.

Active dof during the motion to be synthesized are one rotational freedom in the shoulder and another rotational freedom in the elbow joint. Motion of the hand with respect to the forearm is restricted and hence rotational freedom of the elbow around the forearm axis and all rotational freedoms of wrist are disregarded. Therefore, the system is reduced to a 2R serial planar kinematic chain, i.e. a 2R dyad (Figure 13).

In order to better support this 2R dyad, and constrain the motion to single dof, a closed loop planar linkage is to be designed. Single-dof planar linkages are four link

mechanisms. As one of the dyads of the mechanism is necessarily an RR dyad, some planar linkage types such as the double-slider (PRRP) or Rapson slide (RPRP) are already eliminated. Four-bar and slider crank mechanisms are two possible four-link solutions for this problem. If a slider-crank mechanism is used, the sliding joint might get stuck and construction may be problematic. Hence, a four-bar linkage is chosen as the mechanism to be designed.

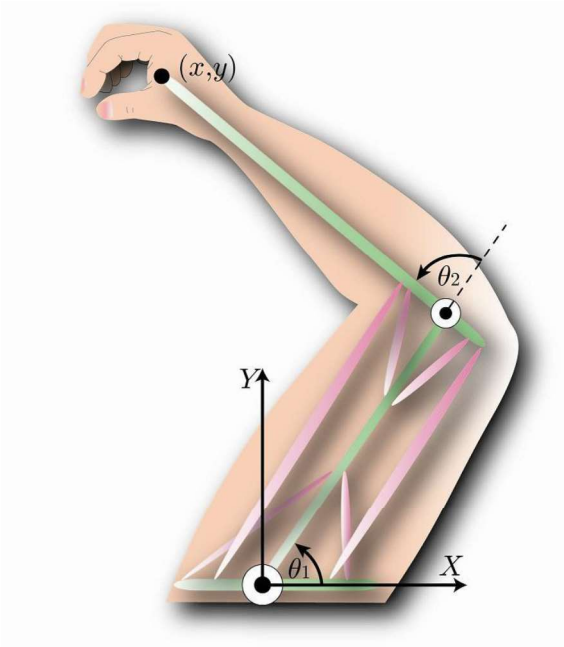

Figure 13. Human Arm as a 2R Serial Planar Kinematic Chain

Two common methods of kinematic synthesis of linkages are analytical and graphical methods. For a given problem, the number of free design parameters is the same for both methods, but change with number of positions or other problem restrictions like prescribed timing [34].

For the motion generation synthesis, an RR dyad has 4 + number of positions - 1 design parameters. The 4 parameters are the vector components of the two vectors constituting the dyad and a crank rotation angle (β in Figure 14) should be the x and y coordinates or the fixed joints, 3 link lengths of the 3 moving links and 3 parameters to define the location of the attachment of the moving body to the coupler link. Synthesis problem is defined by relative positions of the moving body. For each position defined,

two restrictions are added to problem and so the number of free parameters is decreased by two. For a dyad, two position synthesis gives 3, three position synthesis gives 2 and four position synthesis gives 1 independent parameters. For a 2R dyad, the moving joints that make circular motion are called circle points and fixed joints are called center points [34].

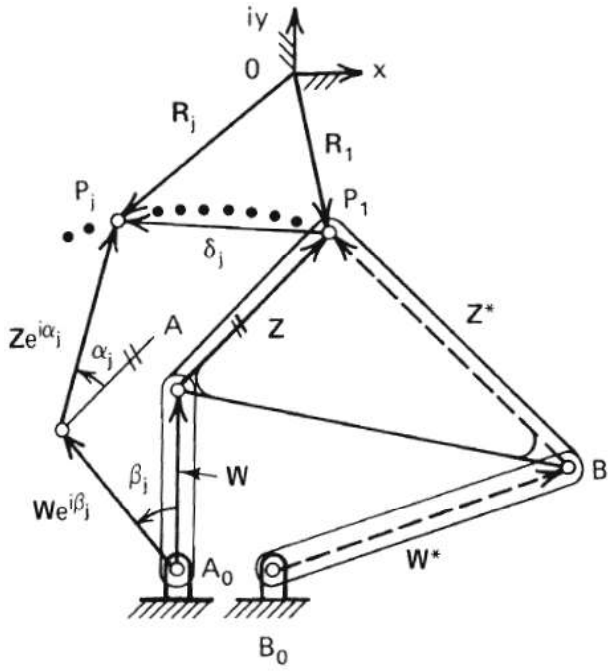

Figure 14. Motion Generation Synthesis of the Four-Bar Linkage [34]

In motion generation synthesis with two or three positions usually the circle points are picked freely and the locations of the center points are found. A moving reference frame is attached to the body to be moved. Circle point is positioned with respect to this moving reference frame and location of the circle point is marked in each position of the moving body. For two or three position synthesis, circle point is selected simply by setting two coordinates in the moving coordinate system. Then, the geometric loci of the points which are equidistant to the circle point locations are determined. In two position synthesis the loci is the perpendicular bisector of the line connecting the two circle points and any point on the line may be chosen to be location of the center point. For three position synthesis, the center point is unique and it is the center of the circle passing through the three circle point locations [34].

Therefore, the circle point is defined by two free parameters for both two and three position synthesis. The location of the center point is freely chosen on a line for two position synthesis which makes the number of free parameters 3. Once the circle point location is chosen, there is no freedom for the selection of the center point. Each dyad is designed following the same procedure. Therefore three position synthesis problem has 4 free design parameters in total.

2.1.2. Problem Specifications and Design

The design problem of this study has limitations other than positions to be synthesized. First limitation is that the 2R comprising the shoulder and elbow joints is already defined. The three positions of the upper arm and forearm are defined with respect to each other as in Figure 15.

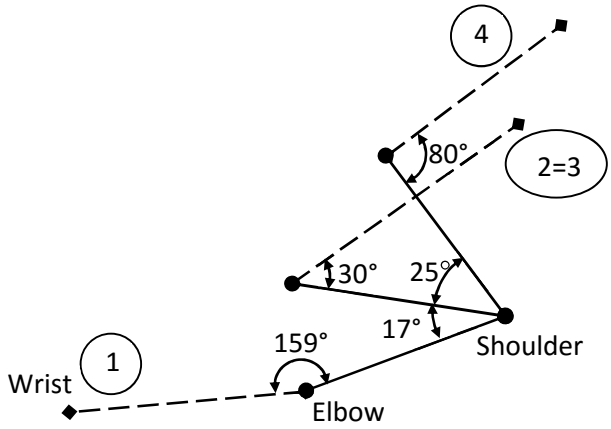

Figure 15. Kinematic Design Problem

Position 2 and 3 are not necessarily coincident. As motion is divided into two sections from 1 to 2 and 3 to 4, problem is not necessarily continuous three positions. Still, one of the dyads, coincident with the upper arm is already defined. The other dyad is to be designed. As an additional limitation, the circle point of the dyad to be designed is placed on the central axis of the forearm instead of any point on the coupler link. This is preferred in order to achieve more compact design. Hence, only one parameter

remains for the dyad design and the length of the coupler, the crank (or rocker) and the fixed link depend on this one parameter. The dyad design is performed in a CAD program and the center point location is chosen such that the wrist point has an approximate straight line path for the exercise in the oblique plane (motion from position 3 to position 4). The mechanism link dimensions are scalable depending on upper arm length which determines the rocker link length. Scalable dimensions are as follows: Fixed: 250 mm, Crank: 150 mm, Coupler: 110.48 mm and Rocker: 280 mm. A CAD model of the mechanism in the vertical and oblique planes are depicted in Figure 16 and Figure 17. Designed mechanism moves from position 1 to 2 and 3 to 4 but position 2 and 3 are not coincident. In order to switch from one exercise to another, mechanism is disassembled on one link and reassembled as the other motion requires.

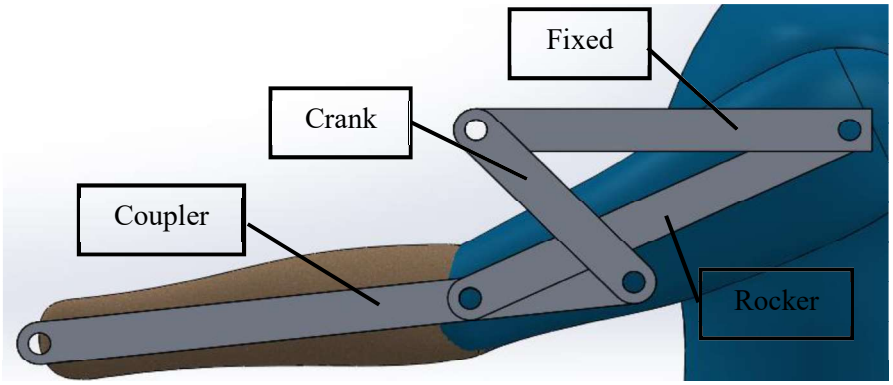

Figure 16. Designed Mechanism in Vertical Plane

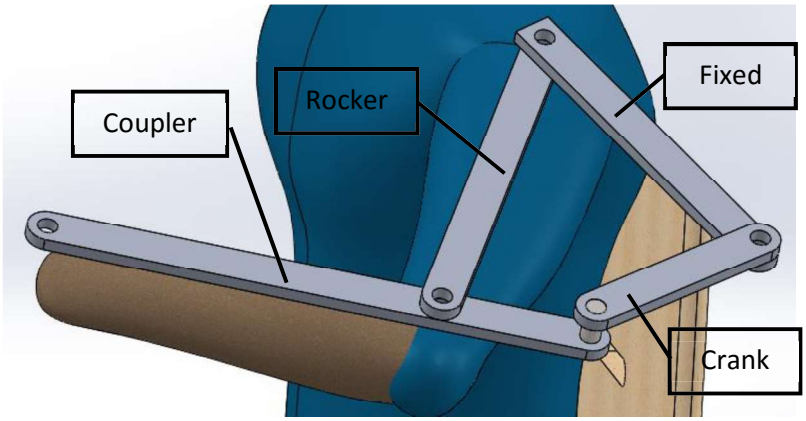

Figure 17. Designed Mechanism in Oblique Plane

2.2. Analysis of the Planar Linkage

The mechanism is exoskeleton type so the links are attached together with the corresponding parts of the arm. Length of bones are calculated according to Sağır's study [35]. Sağır measured total body height of people and their bone lengths through radiography. The purpose of the study was to estimate total body lengths of bodies found in the archeological sites. Measurements were taken from patients in hospitals and estimation formulations are introduced to calculate total body length from bone length. Only the upper arm length is needed in this study. Therefore, mathematical relation between body height (BH) and Humerus bone is formulated as:

BH = 25.12 x Humerus + 870.7 mm

This formulation is used for calculating the length of Humerus from body height:

Humerus = BH / 25.12 – 346.6 mm

Sample calculations is done for a person who is 1700 mm tall. Corresponding upper arm (rocker) length is 330.1 mm and scaled link lengths are calculated as; fixed link: 294.8 mm, crank: 176.9 mm and coupler: 130.3 mm.

Mass and position of mass center for arm sections are estimated according to study by Plagenhoef et al. [36]. According to the study, upper arm mass is 3.25% of total body mass (BM) for male and 2.9% for female subjects. Forearm mass is 1.87% of total BM for male and 1.57% for female subjects. Even mass fraction of hand changes by gender as 0.65% for male and 0.50% for female. For sample calculations, a patient of 100 kg BM is assumed to be subject as the system is supposed to work with any patient. A person with 100 kg BM and 1.70 m BH has 34.6 Body Mass Index (BMI) which is considered to be obese. The choice of 100 kg BM is considered to be an upper limit for the mechanism and the static force analysis is done for the highest expected load.

The motion occurs in two different planes. Although the last position of one motion is the same with the beginning of the other, force balance is different due to changing effect of gravity. First, the analysis is performed for a motor connected to the crank. Motor torque balances more gravitational force in the vertical plane.

2.2.1. Virtual Work Model

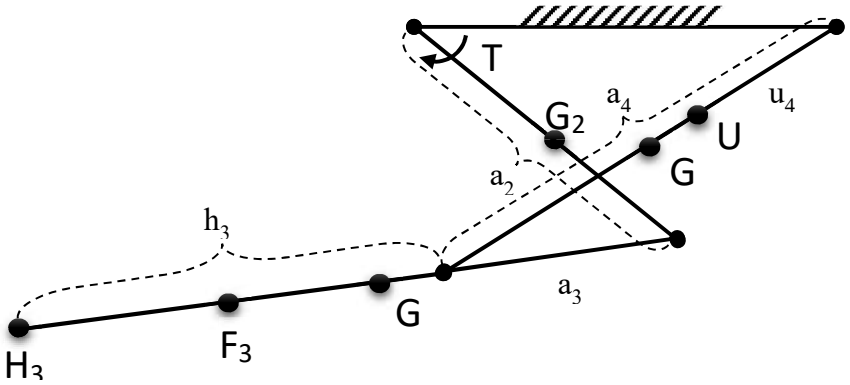

Figure 18. Virtual Work Analysis Parameters

Ignoring all inertial forces as motion is slow, only gravitational forces and cable tension will be applying on mechanism. Figure show the location of mass centers of all objects in the loop. G_is are mass centers of links. They are assumed to be in the middle of links and coupler is considered together with its extension for this case. U_4 is the mass center of upper arm and has a subscript of 4 as it moves together with 4th link, rocker. Similarly, F_3 represents mass center of fore arm and H_3 represents that of hand. Positions will only be considered vertical for mass centers as gravitational force has no horizontal component.

$$G_{2y}=\frac{a_2}{2}\sin\theta_2 \Rightarrow \delta G_{2y}=\frac{a_2}{2}\cos\theta_2\delta\theta_2 \tag{2.1}$$

$$G_{3y}=a_2\sin\theta_2+\frac{a_3+h_3}{2}\sin\theta_3 \Rightarrow \delta G_{3y}=a_2\cos\theta_2\delta\theta_2+\frac{a_3+h_3}{2}\cos\theta_3\delta\theta_3 \tag{2.2}$$

$$G_{4y}=\frac{a_4}{2}\sin\theta_4 \Rightarrow \delta G_{4y}=\frac{a_4}{2}\cos\theta_4\delta\theta_4 \tag{2.3}$$

$$F_{3y}=a_2\sin\theta_2+(a_3+f_3)\sin\theta_3 \Rightarrow \delta F_{3y}=a_2\cos\theta_2\delta\theta_2+(a_3+f_3)\cos\theta_3\delta\theta_3 \tag{2.4}$$

$$H_{3y}=a_2\sin\theta_2+(a_3+h_3)\sin\theta_3 \Rightarrow \delta H_{3y}=a_2\cos\theta_2\delta\theta_2+(a_3+h_3)\cos\theta_3\delta\theta_3 \tag{2.5}$$

$$U_4=u_4\sin\theta_4 \Rightarrow \delta U_4=u_4\cos\theta_4\delta\theta_4 \tag{2.6}$$

When all equations are divided by $\delta\theta_2$, $\frac{\delta\theta_4}{\delta\theta_2}$ and $\frac{\delta\theta_3}{\delta\theta_2}$ is required to find explicit expression for all parameters. Derivative of loop closure equations gives these two key multipliers:

$$a_2e^{i\theta_2}+a_3e^{i\theta_3}=a_1+a_4e^{i\theta_4}\Rightarrow i\delta\theta_2a_2e^{i\theta_2}+i\delta\theta_3a_3e^{i\theta_3}=i\delta\theta_4a_4e^{i\theta_4} \quad (2.7)$$

$$-\delta\theta_2a_2\sin\theta_2=\delta\theta_3a_3\sin\theta_3-\delta\theta_4a_4\sin\theta_4 \quad (2.8)$$

$$\delta\theta_2a_2\cos\theta_2=-\delta\theta_3a_3\cos\theta_3+\delta\theta_4a_4\cos\theta_4 \quad (2.9)$$

$$\begin{pmatrix} a_3\sin\theta_3 & -a_4\sin\theta_4 \\ -a_3\cos\theta_3 & a_4\cos\theta_4 \end{pmatrix}^{-1}\begin{pmatrix} -a_2\sin\theta_2 \\ a_2\cos\theta_2 \end{pmatrix}=\begin{pmatrix} \frac{\delta\theta_3}{\delta\theta_2} \\ \frac{\delta\theta_4}{\delta\theta_2} \end{pmatrix} \quad (2.10)$$

$$\Rightarrow\frac{\delta\theta_4}{\delta\theta_2}=\frac{a_2\sin(\theta_3-\theta_2)}{a_4\sin(\theta_3-\theta_4)}\ \&\ \frac{\delta\theta_3}{\delta\theta_2}=\frac{a_2\sin(\theta_4-\theta_2)}{a_3\sin(\theta_3-\theta_4)} \quad (2.11)$$

$$T\delta\theta_2=g(m_2\delta G_{2y}+m_3\delta G_{3y}+m_4\delta G_{4y}+m_u\delta U_{4y}+m_f\delta F_{3y}+m_h\delta H_{3y}) \quad (2.12)$$

$$\Rightarrow T=\frac{g(m_2\delta G_{2y}+m_3\delta G_{3y}+m_4\delta G_{4y}+m_u\delta U_{4y}+m_f\delta F_{3y}+m_h\delta H_{3y})}{\delta\theta_2} \quad (2.13)$$

Force analysis is performed for link lengths mentioned above. Masses are represented in equations by m_i. Link lengths are a_1 = 294.8 mm, a_2 = 176.9 mm, a_3 = 130.3 mm, f_3 = 142.0 mm (mass center distance of the front arm from the elbow), h_3 = 375.9 mm (mass center distance of the hand from the elbow), u_4 = 143.9 mm (mass center distance of the upper arm from the shoulder center) and a_4 = 330.1 mm. Mass of links and body parts are m_2 = 0,212 kg (crank mass), m_3 = 0,607 kg (coupler mass), m_4 = 0,396 kg (rocker mass), m_u = 3,25 kg (upper arm mass), m_f = 1,87 kg (front arm mass) and m_h = 0,65 kg (hand mass).

The results by virtual work method is shown in Figure 19 & Figure 20.

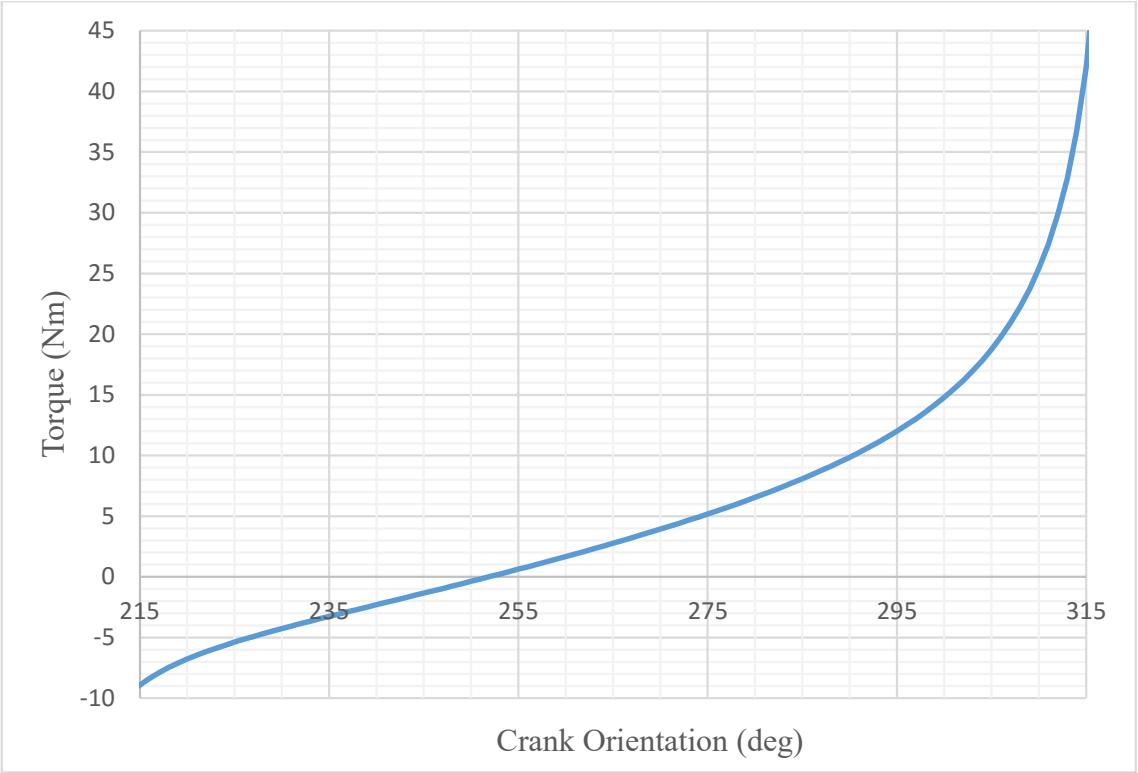

Figure 19. Resultant Crank Torque Requirement for Motion in Vertical Plane

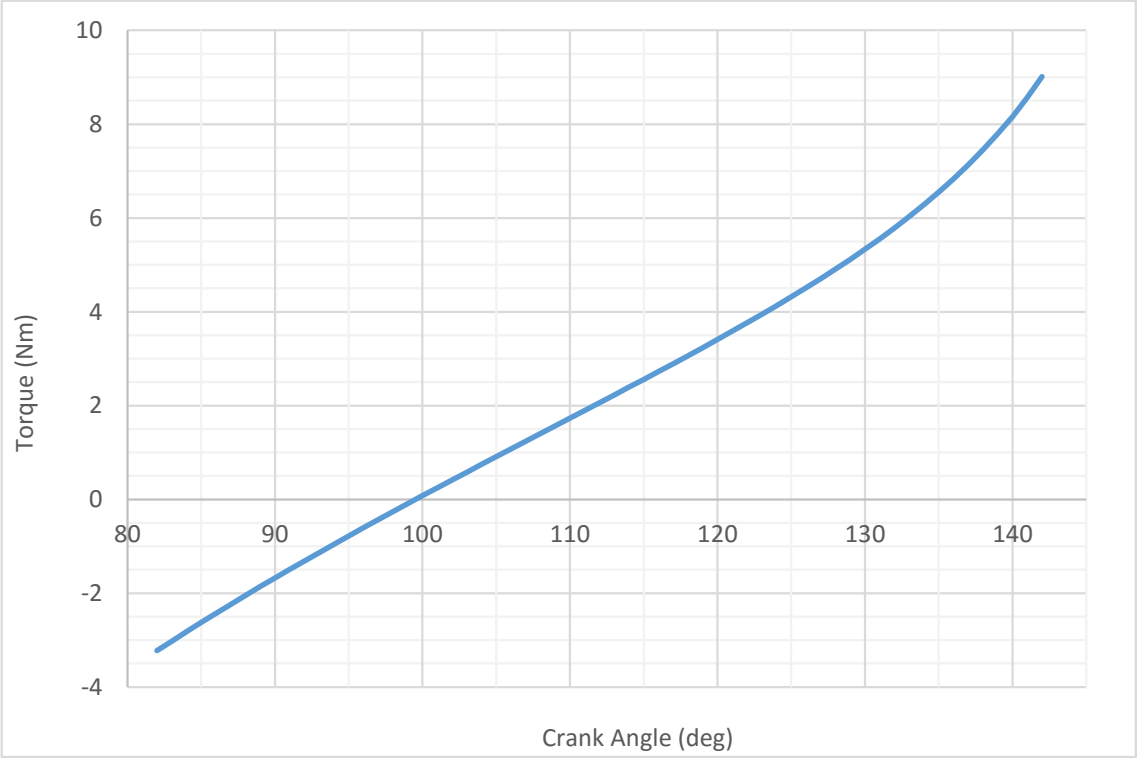

Figure 20. Resultant Crank Torque Requirement for Motion in Oblique Plane

The torque requirement for the motion in the oblique plane has an acceptable distribution. However, due to poor transmission angle at the beginning of the motion in vertical plane, where crank angle is 315° and transmission angle is 21.14°, crank actuation is not practical. Solution to the actuation problem is explained in the next chapter.

2.3. Changing the Motion Plane of the Four-Bar Linkage

2.3.1. Problem Specifications & Type Synthesis

The planar mechanism is designed to support two exercise motions. Orientation of the fixed link of the planar linkage needs to be reconfigured before switching to the other motion. Fixed link stay horizontal (parallel to the ground) during the motion in vertical plane (Figure 16). For the motion in the oblique plane, orientation of the fixed link is not parallel to any ground frame axes. The plane of motion makes 30° with the ground level. The angle between the fixed link and the vertical backplane (the surface of chair which the patients lean their back) is also 30°. The shoulder joint center needs to remain in position, though there should be room for adjustment as the shoulder joint is not fixed to the chest.

Therefore, problem definition of this part is two position synthesis in space. The four-bar mechanism frame is the body to be moved from one position to the other. The kinematic element on the mechanism frame that forms the revolute joint with rocker link is assumed to be coincident with the shoulder center. Achieving a simple rotation around the shoulder joint meets the requirement of shoulder joint to maintain its position.

2.3.2. Kinematic Design

The simplest motion between two positions in plane is rotation around a point. A body may move from one position to another by pure rotation. The point around which the body is rotated, the pole, may be anywhere in the plane. Location of the pole for

pure translational motions is theoretically infinitely away from the body, still in the plane.

Similarly, simplest motion between two positions in space is rotation around and translation along a screw axis. The mechanism is attached to the arm and they move together. Therefore shoulder center should not move. Since there is a common stationary point in both positions, the screw motion has to be a pure rotation and hence screw axis is a stationary rotation axis which passes through the shoulder center.

Similar to finding the center point for two positions of a plane, two random points on the body are picked. The lines connecting the two different position of each point are drawn. A perpendicular bisector plane is drawn for both line segments. The planes are created in 3D CAD environment with two basic properties; coincident with midpoint of line segment and perpendicular to the line segment. Finally, the intersection line of the two planes gives the unique axis of rotation for pure rotation between two positions in space. Resultant orientation of the revolute joint axis is found as $X(-60°)\cdot Y(-\alpha)\cdot(0\ 0\ 1)^T$, where X() and Y() are standard transformation matrices about the x- and y-axes shown in and $\alpha = \tan^{-1}(2/3)$.

CHAPTER 3

ACTUATION SOLUTIONS

The motion of the mechanism is modelled as starting from the lowermost position of the exercise in the vertical plane and continue from the same pose in the oblique plane. So, the mechanism starts the motion in the vertical plane with a transmission angle of 21°. As shown in Chapter 2, torque requirement is much higher in a small range of crank rotation if the crank is the input link. Total amount of rotation of the crank is limited to 96° for motion in vertical plane and 39° for motion in oblique plane, which points out poor mechanical advantage characteristics. In order to overcome these problems, alternative actuation means are proposed and analyzed in this chapter.

3.1. Addition of an Extra Dyad

This solution arose from the fact that the higher torque is required for a limited section of the motion. The purpose of this solution is to increase the amount of rotation of the actuator in the section where the crank torque requirement is high. Therefore, for the same amount of work, actuator torque requirement will be lower as the actuator displacement is increased.

3.1.1. Methodology

The mechanism is actuated with an additional link group. Crank of the designed four bar mechanism could be used as the rocker of the newly formed loop. The four-bar mechanism is made of three moving links and a base or fixed link. Newly designed four-bar loop has the same base and has the crank of the main four-bar as its rocker. As the firstly designed four-bar is not altered, the motion of the four-bar is kept the same. New dyad comprises two additional links to the system. Actuator will be placed on the new crank. Motion in vertical plane is more problematic, so the dyad is designed to achieve dead center position in this motion. Because, near the dead-center position, the

ration of the crank speed to the rocker speed is maximized, hence the amount of crank rotation is relatively large for the same amount of rotation of the rocker. The resulting six-link mechanism is shown in Figure 21 and Figure 22

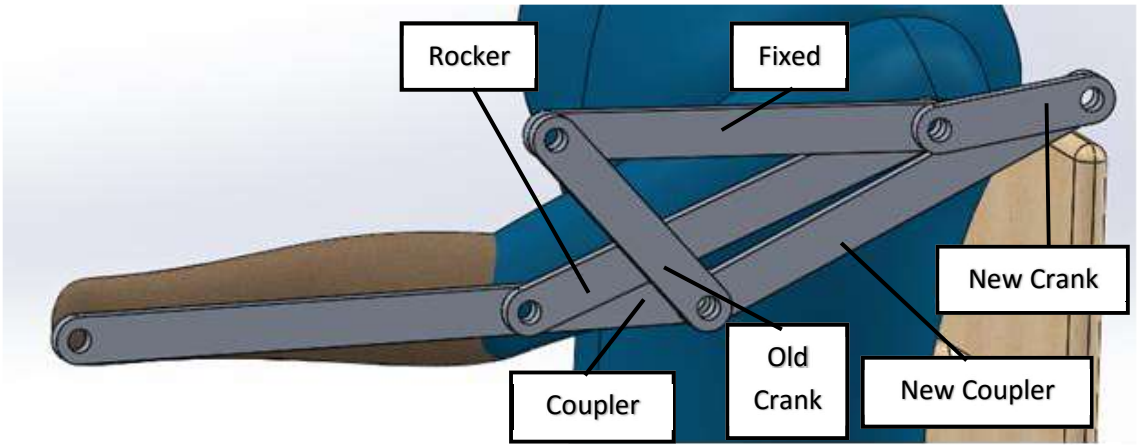

Figure 21. Mechanism with Extra Dyad in Vertical Plane

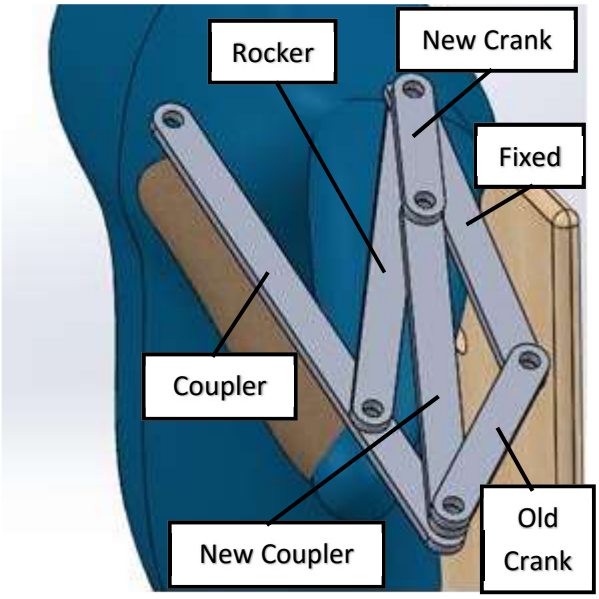

Figure 22. Mechanism with Extra Dyad in Oblique Plane

3.1.2. Analysis Results

Similar to the four-bar mechanism analysis, the system is analyzed in Excel environment analytically. The amount of crank rotation for the motion in vertical plane is 142°, which is better in terms of mechanical advantage compared to the 96° crank rotation. For the motion in oblique plane, 98° crank rotation is achieved in return of 60° old crank rotation.

Analysis results show that the problem of sudden increase in the torque has been resolved and the torque requirement variation is smoothened (Figure 23-24). The crank angle in Figure 23-24 belong to the new crank of the additional dyad. A prototype of the resulting six-link mechanism is built. When the mechanism is worn by several people, two important problems are observed. First problem is the motion limit of folded arm, position 2 or 3, is not usually practically achievable due to physiological limitations of human arm. Other problem is that back drivability of the mechanism is practically much worse than firstly designed four-bar mechanism.

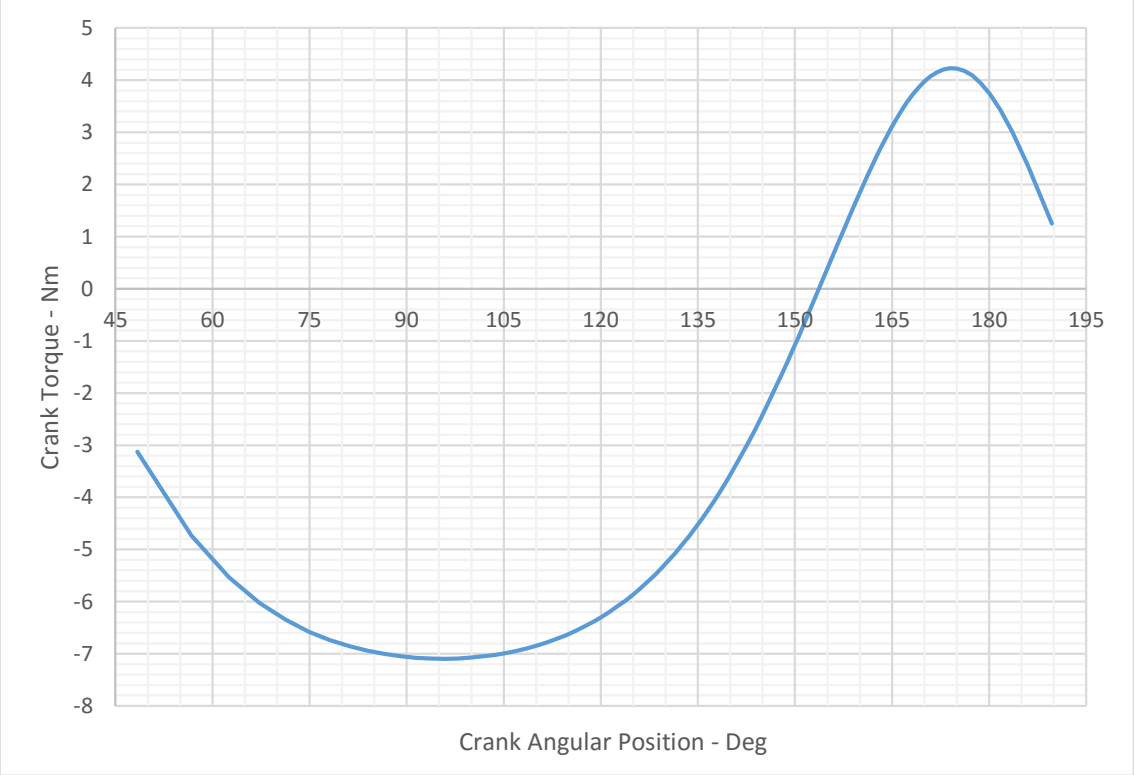

Figure 23. Analysis Result for Motion in Oblique Plane

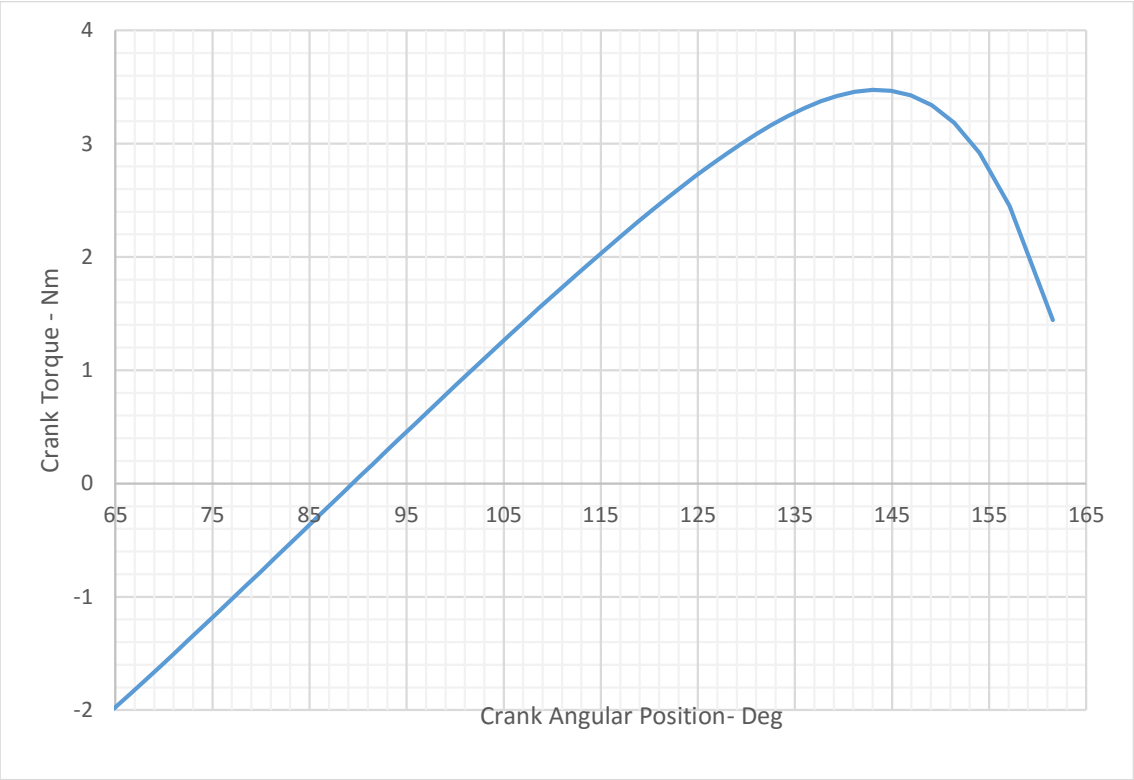

Figure 24. Analysis Result for Motion in Vertical Plane

3.2. Cable Actuation

The problems observed with the 6-link model required that the motion parameters will be redefined and another actuation method is to be followed. First, mechanism is modified to achieve new limits of motion and requirements of cable drive. Previous mechanism required reassembling between two motions. Cable drive is not practical in this case because cable drive elements also need to be reassembled during the re-orientation. Mechanism would become impractical with this design. First, motion problem is redefined as three position synthesis. After achieving continuous motion between all positions, cable drive is designed. In this section, cable drive method is mentioned in general before introducing the design procedure. Finally, force analysis is performed with two methods, virtual work and free body diagram, and intermediate pulleys are designed according to iterative analysis results.

3.2.1. Mechanism Re-Design

In order to achieve continuity throughout both motions combined, problem is defined to be three position synthesis as shown in Figure 25. Orientations of upper and forearm are defined with respect to horizontal axis instead of with respect to previous position. Motion limits have changed according to practical measurements.

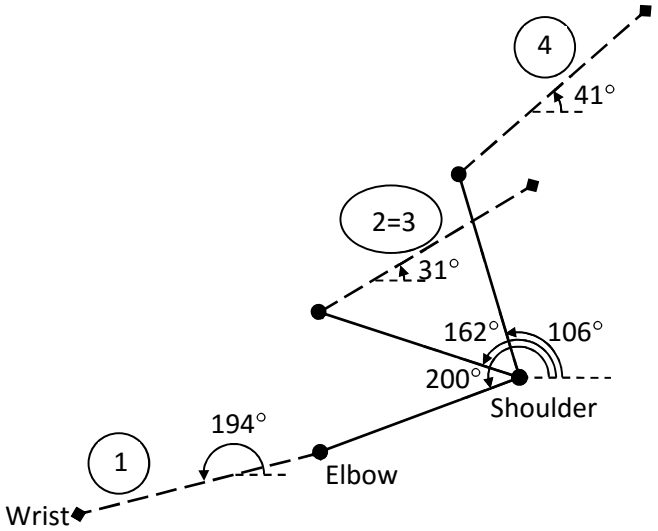

Figure 25. New Mechanism Design Positions

The three position synthesis is explained in Chapter 2. Mechanism is synthesized graphically. The new designed mechanism has unscaled link lengths as fixed link: 250.36 mm, crank: 162.78 mm, coupler: 171.38 mm and rocker: 280 mm.

3.2.2. Cable Drive Solution

Cable actuation, also known as tendon drive, is simply actuating a rigid body or a system of rigid bodies by pulling one or more cables. Cable actuation has several advantages. For almost all applications, actuators are placed on the base and forces are transferred to moving bodies through cables. By this way, moving mass is reduced.

Moving masses of a mechanical system are rigid links and motors placed at the joints. Replacing motors with pulleys, which are much lighter elements, decreases moving mass and increases dynamic performance of the system and/or decrease energy requirement. For a parallel manipulator, moving masses are rigid links including the mobile platform. Motors are mostly located at the base and rigid links are driven to position the platform. Cable driven parallel manipulators are systems in which rigid links connecting the base and the platform are cables. Cables are quite lighter than rigid links and therefore moving mass is considerably decreased.

Cable drive is preferred in exoskeleton type rehabilitation robots in order to achieve a compact design. Placing motors on each joint is not comfortable or even not applicable for arm exoskeleton robots. Cable drive is frequently referred as tendon drive for exoskeleton rehabilitation robots as the working principle is very similar. Cable length is changed by an actuator.

A major disadvantage of cable drive is single direction of actuation. Cables are elastic elements which may only pull but not push. Bowden cables (Figure 26) are invented in order to achieve pull and push function together.

Figure 26. Bowden Cable [37]

In the following subsections a system with cable-drive is designed for the exoskeleton mechanism, where the cable drive ensures the part of the motion against gravity with a relatively smooth actuation torque requirement. The actuation system is designed to actuate the mechanism forward and backward with a closed loop cable. During the motion in the vertical plane, the mechanism needs to overcome the gravitational forces as the hand moves from lower level (position 1 in Figure 25) to upper level (position 2). During this motion, if there is any, spasm forces work in favor

of the mechanism. However, during the reverse motion (from position 2 to 1), the gravitational forces does positive work for the mechanism, while the spasm forces are to be overcome. Note that spasm forces are assumed to be less than (about at most %20) the gravitational forces. For the motion in the oblique plane, the level of the center of gravity of the arm does not change much, but the analyses show that the center elevates during the motion from position 3 to position 4. The mechanism actuator does work against the gravitational plus the spasm forces during this motion. However, note that since the level of the center of gravity does not change much, the motor torque requirement is much less for the motion in the oblique plane then the requirement for the motion in the vertical plane. Therefore, the critical motion which effects the actuation design is the motion in the vertical plane. For these reasons, the mechanism is actuated in one direction (From position 1 to 2 and then from position 3 to 4) with cable and the gravitational forces are considered to be the only forces to be overcome by the actuation force during the analyses.

3.2.3. Design of the Cable Drive

In this subsection first the kinematic analysis or the mechanism to be actuated is performed in order to determine a proper attachment point for the cable. Then the design of the cable-drive system is presented.

3.2.3.1. Kinematic Analysis of the Mechanism

The mechanism is a planar four-bar mechanism (Figure 27). For analyzing the motion of the mechanism, θ_{12} is taken as the independent parameter of the mechanism.

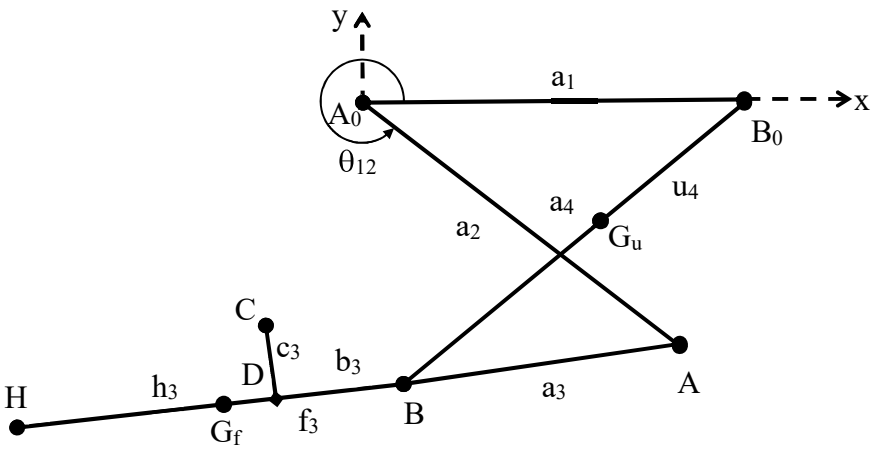

Figure 27. Kinematic diagram of the mechanism

$|A_0B_0| = a_1$, $|A_0A| = a_2$, $|AB| = a_3$, $|B_0B| = a_4$, $|BD| = b_3$, $|DC| = c_3$, $|BH| = h_3$

For the kinematic analysis, A_0 is taken as the origin, position of point A is given as:

$$A_x = a_2 \cos\theta_{12} \tag{3.1}$$

$$A_y = a_2 \sin\theta_{12} \tag{3.2}$$

Then, θ_{14} is found as follows:

$$s = \sqrt{(A_x - a_1)^2 + A_y^2} \tag{3.3}$$

$$\phi = \text{Atan2}(a_1 - A_x; A_y) \tag{3.4}$$

$$\xi = \cos^{-1}\frac{s^2 + a_4^2 - a_3^2}{2sa_4} \tag{3.5}$$

$$\theta_{14} = \phi - \xi \tag{3.6}$$

Position of point B can be found as:

$$B_x = a_1 + a_4 \cos\theta_{14} \tag{3.7}$$

$$B_y = a_4 \sin\theta_{14} \tag{3.8}$$

θ_{13} is found using coordinates of B:

$$\theta_{13} = \text{Atan2}(B_x - A_x; B_y - A_y) \tag{3.9}$$

The hand position is given as:

$$H_x = A_x + (a_3 + h_3)\cos\theta_{13} \tag{3.10}$$

$$H_y = A_y + (a_3 + h_3)\sin\theta_{13} \tag{3.11}$$

For the velocity analysis the derivative of the loop closure equations of the four-bar mechanism is taken. The loop closure equations:

$$a_2\cos(\theta_{12})+a_3\cos(\theta_{13})=a_1+a_4\cos(\theta_{14}) \tag{3.12}$$

$$a_2\sin(\theta_{12})+a_3\sin(\theta_{13})=a_4\sin(\theta_{14}) \tag{3.13}$$

Differentiating gives ω_{13} and ω_{14} in terms of ω_{12}:

$$\omega_{12}a_2\sin(\theta_{12})+\omega_{13}a_3\sin(\theta_{13})=\omega_{14}a_4\sin(\theta_{14}) \tag{3.14}$$

$$\omega_{12}a_2\cos(\theta_{12})+\omega_{13}a_3\cos(\theta_{13})=\omega_{14}a_4\cos(\theta_{14}) \tag{3.15}$$

$$\Rightarrow\begin{bmatrix} a_4\sin(\theta_{14}) & -a_3\sin(\theta_{13}) \\ a_4\cos(\theta_{14}) & -a_3\cos(\theta_{13}) \end{bmatrix}\begin{bmatrix}\omega_{14}\\ \omega_{13}\end{bmatrix}=\begin{bmatrix}\omega_{12}a_2\sin(\theta_{12})\\ \omega_{12}a_2\cos(\theta_{12})\end{bmatrix} \tag{3.17}$$

$$\omega_{13}=\frac{a_2\sin(\theta_{14}-\theta_{12})}{a_3\sin(\theta_{13}-\theta_{14})}\omega_{12}=g_{13}\omega_{12} \tag{3.18}$$

$$\omega_{14}=\frac{a_2\sin(\theta_{13}-\theta_{12})}{a_4\sin(\theta_{13}-\theta_{14})}\omega_{12}=g_{14}\omega_{12} \tag{3.19}$$

where g_{13} and g_{14} are velocity influence coefficients, which are functions of the position variables only, i.e. $g_{13}(\theta_{12})$ and $g_{14}(\theta_{12})$ [38]. Taking the derivatives of the velocities:

$$\alpha_{13}=g_{13}\alpha_{12}+\frac{dg_{13}}{dt}\omega_{12}=g_{13}\alpha_{12}+\frac{dg_{13}}{d\theta_{12}}\omega_{12}{}^2=g_{13}\alpha_{12}+h_{13}\omega_{12}{}^2 \tag{3.20}$$

$$\alpha_{14}=g_{14}\alpha_{12}+\frac{dg_{14}}{dt}\omega_{12}=g_{14}\alpha_{12}+\frac{dg_{14}}{d\theta_{12}}\omega_{12}{}^2=g_{14}\alpha_{12}+h_{14}\omega_{12}{}^2 \tag{3.21}$$

where $h_{13}=dg_{13}/d\theta_{12}$ and $h_{14}=dg_{14}/d\theta_{12}$ are acceleration influence coefficients. h_{13} and h_{14} are given by

$$\begin{aligned} h_{13}&=\frac{a_2}{a_3}\frac{\cos(\theta_{14}-\theta_{12})(g_{14}-1)\sin(\theta_{13}-\theta_{14})-\sin(\theta_{14}-\theta_{12})\cos(\theta_{13}-\theta_{14})(g_{13}-g_{14})}{\sin^2(\theta_{13}-\theta_{14})}\\ &=\frac{a_4g_{14}{}^2}{a_3\sin(\theta_{13}-\theta_{14})}-\frac{g_{13}^2}{\tan(\theta_{13}-\theta_{14})}-\frac{g_{13}}{\tan(\theta_{14}-\theta_{12})}\end{aligned} \tag{3.22}$$

$$\begin{aligned} h_{14}&=\frac{a_2}{a_4}\frac{\cos(\theta_{13}-\theta_{12})(g_{13}-1)\sin(\theta_{13}-\theta_{14})-\sin(\theta_{13}-\theta_{12})\cos(\theta_{13}-\theta_{14})(g_{13}-g_{14})}{\sin^2(\theta_{13}-\theta_{14})}\\ &=-\frac{a_3}{a_4\sin(\theta_{13}-\theta_{14})}g_{13}{}^2+\frac{1}{\tan(\theta_{13}-\theta_{14})}g_{14}{}^2-\frac{a_2}{a_4}\frac{\cos(\theta_{13}-\theta_{12})}{\sin(\theta_{13}-\theta_{14})}\end{aligned} \tag{3.23}$$

Up to here all variables are formulated in terms of θ_{12}, θ_{13} and θ_{14} for ease of the calculations, however, when the system is cable-driven, the mechanism is actuated from point C. Coordinates and speed of point C:

$$x_C = a_2\cos(\theta_{12}) + (a_3 + b_3)\cos(\theta_{13}) + c_3\sin(\theta_{13}) \tag{3.24}$$

$$y_C = a_2\sin(\theta_{12}) + (a_3 + b_3)\sin(\theta_{13}) - c_3\cos(\theta_{13}) \tag{3.25}$$

$$\dot{x}_C = \left\{-a_2\sin(\theta_{12}) + \left[c_3\cos(\theta_{13}) - (a_3 + b_3)\sin(\theta_{13})\right]g_{13}\right\}\omega_{12} = u_C\omega_{12} \tag{3.26}$$

$$\dot{y}_C = \left\{a_2\cos(\theta_{12}) + \left[(a_3 + b_3)\cos(\theta_{13}) + c_3\sin(\theta_{13})\right]g_{13}\right\}\omega_{12} = v_C\omega_{12} \tag{3.27}$$

$$\dot{s}_C = \sqrt{\dot{x}_C{}^2 + \dot{y}_C{}^2} = \sqrt{u_C{}^2 + v_C{}^2}\,\omega_{12} = g_C\omega_{12} \tag{3.28}$$

where

$$g_C = \sqrt{a_2{}^2 + g_{13}{}^2\left(c_3{}^2 + \left(a_3 + b_3\right)^2\right) + 2g_{13}a_2\left[c_3\sin\left(\theta_{13} - \theta_{12}\right) + \left(a_3 + b_3\right)\cos\left(\theta_{13} - \theta_{12}\right)\right]} \tag{3.29}$$

The cable speed $\dot{s}_C$ is assumed to be constant during the motion. Then

$$\ddot{s}_C = 0 = g_C\alpha_{12} + \frac{dg_C}{d\theta_{12}}\omega_{12}{}^2 = g_C\alpha_{12} + h_C\omega_{12}{}^2 \tag{3.30}$$

where

$$h_c = \frac{g_{13}h_{13}\left(c_3{}^2 + \left(a_3 + b_3\right)^2\right) + h_{13}a_2\left[c_3\sin\left(\theta_{13} - \theta_{12}\right) + \left(a_3 + b_3\right)\cos\left(\theta_{13} - \theta_{12}\right)\right]}{g_c} + \frac{g_{13}a_2\left(g_{13} - 1\right)\left[c_3\cos\left(\theta_{13} - \theta_{12}\right) - \left(a_3 + b_3\right)\sin\left(\theta_{13} - \theta_{12}\right)\right]}{g_c} \tag{3.31}$$

α_{12} can be determined as

$$\alpha_{12} = -\frac{h_C\omega_{12}{}^2}{g_C} \tag{3.32}$$

3.2.3.2. Cable Drive Optimization Procedure

Cable drive is preferred for this application to overcome actuation requirements near singular configurations of the mechanism. The most critical pose is the beginning of motion in the vertical plane, where the hand is at the lowest position, because the mechanism is near singular position. Crank torque requirement increases near singularity.

However, cable actuation may add the mechanism an optimized drive. Cable is wrapped around a pulley and mechanism is pulley in one direction in this method. The component of tension force in the direction of motion of cable attachment point actuates the system while the other component only increase joint reaction forces. Therefore, it is desired to obtain a point which make a straight line motion in the direction where the cable is oriented. Cable tip attached to any point on rocker or crank may follow an arc shaped path as the two links make pure rotation. Therefore, the only flat line or similar path may be achieved on coupler link. The location of the cable attachment point C on the coupler link AH provides two design parameters: b_3 and c_3. Position of C is formulated as:

$$C_x = A_x + (a_3 + b_3)\cos\theta_{13} - c_3\sin\theta_{13} \quad (3.33)$$

$$C_y = A_y + (a_3 + b_3)\sin\theta_{13} + c_3\cos\theta_{13} \quad (3.34)$$

First design was a direct connection between motor pulley and point C (Figure 28). Design requirement is to achieve a flat curve so that the angle between cable tension and direction of motion of point C will remain small for better transmission. Procedure for defining b_3 and c_3 is applied in excel. First, the motion is divided into sections of 1° crank angle. Point C trajectory is divided into line segments by this division. Then, the angle between each line segment is calculated in radians as the straightness error of the trajectory. Finally, square of errors summed. The greater the number obtained as sum, the more curved the line is. The location of point C is limited to a region where $-a_3 \leq b_3 \leq h_3$ and $-200 \text{ mm} \leq c_3 \leq 200 \text{ mm}$. The algorithm is applied on the region with equally distanced points. However, the only acceptable result is obtained near point B which is a point on rocker link and make a short arc shaped trajectory.

Another way to optimize the trajectory of C is to divide it into straight sections. Each straight section has its own pulley and as mechanism moves, point C on coupler link pass through each straight section, go around a pulley such that cable lose contact with that pulley and goes for next straight section. A sample illustration of three intermediate pulleys example is shown in Figure 29.

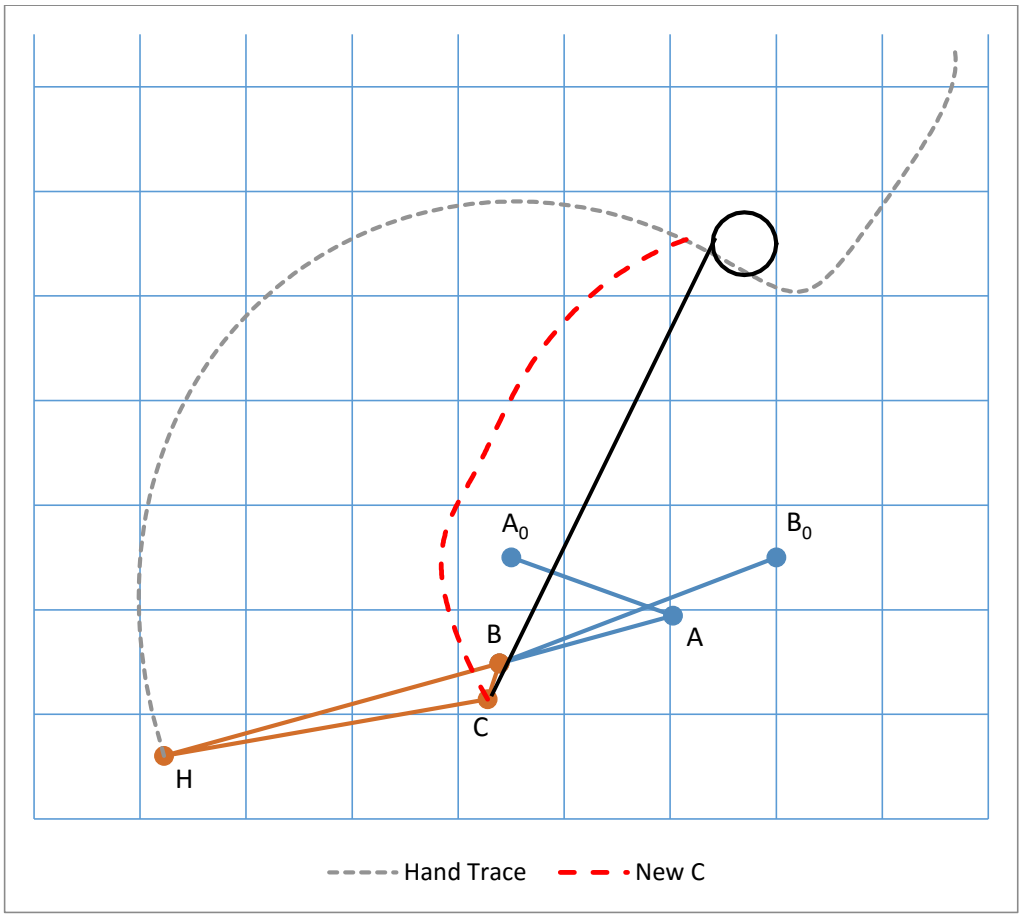

Figure 28. Cable Drive with a Single Motor Pulley

In this set of pulleys, in addition to location of point C and position and radius of the motor pulley, position and radius of the intermediate pulleys are also design parameters. Optimum location for point C on coupler is determined same way it is optimized for solution without intermediate pulleys. However, motion is analyzed in parts. Three excel sheets present the three sections of trajectory and straight path test is applied for same limits of values of b_3 and c_3. In order to iterate in a smaller region, limiting values are set to better resulting zone within the limits defined for b_3 and c_3 at the beginning. New limits are 0 mm $\leq b_3 \leq$ 80 mm and -50 mm $\leq c_3 \leq$ 50 mm. Then, with an initial values of b_3 = 25 mm and c_3 = -25 mm, location of point C is optimized using half millimeter iterations for simplicity in construction. Final location of point C is given by b_3 = 25.5 mm and c_3 = –27 mm.

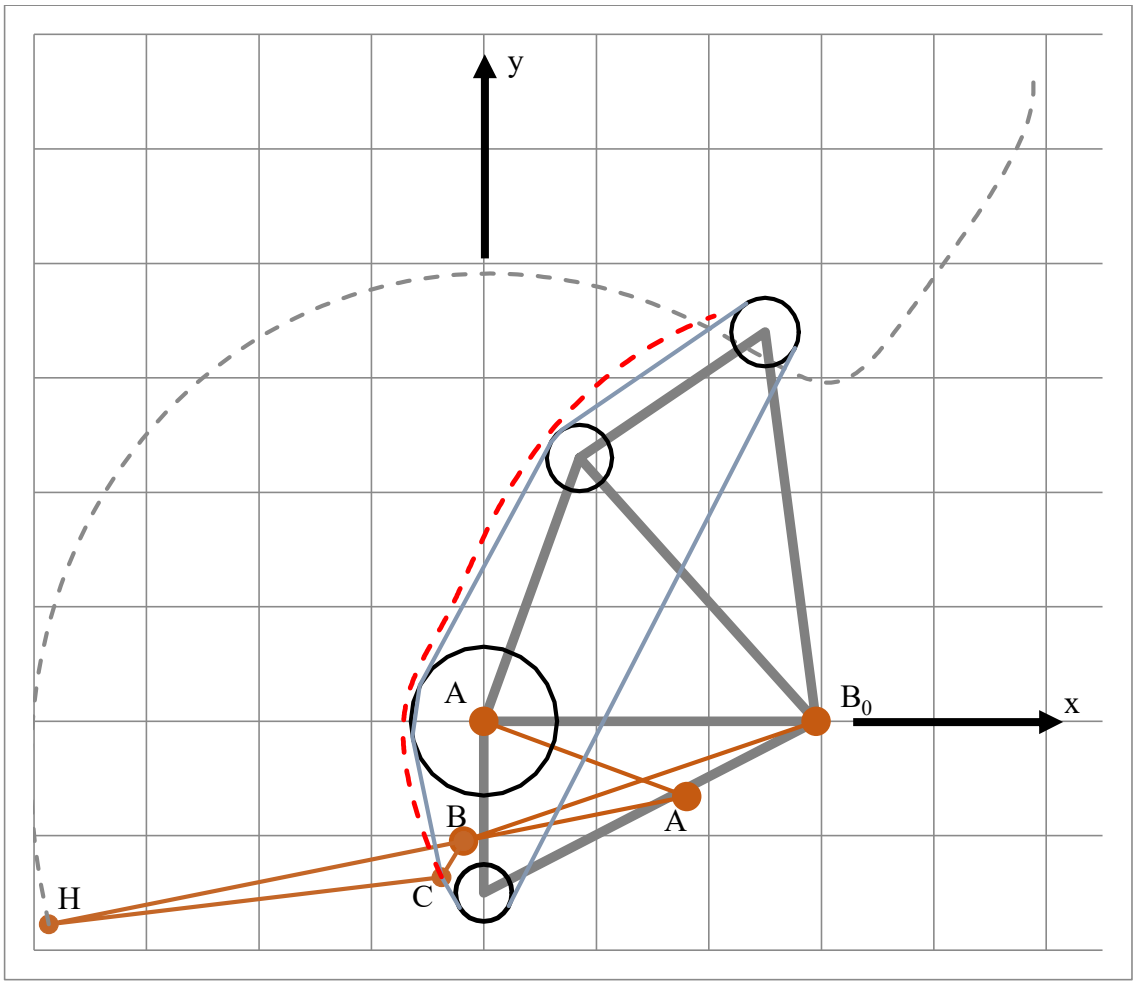

Figure 29. Cable Drive with Multiple Pulleys

3.2.3.3. Kinematic Analysis Parameters of Cable Drive

In order to define the angle of cable connection, first angle of tangent lines between pulleys need to be determined. Referring to Figure 30, the slopes of the cable sections between the pulleys are calculated as follows:

$$d_{ij}=\sqrt{(x_j-x_i)^2+(y_j-y_i)^2} \tag{3.35}$$

$$\varphi_{ij}=\mathrm{Atan2}(x_j-x_i;y_j-y_i) \tag{3.36}$$

$$\gamma_{ij}=\mathrm{Asin}\left(\frac{r_i-r_j}{d_{ij}}\right) \tag{3.37}$$

$$\theta_{p_{ij}}=\varphi_{ij}-\gamma_{ij} \tag{3.38}$$

Where d_{ij} is the distance between central axes of pulleys, x_i or y_i are corresponding coordinate variables and r_i is the radius of i^{th} pulley, θ_{pij} is the orientation angle of the tangent line between i^{th} and j^{th} pulley.

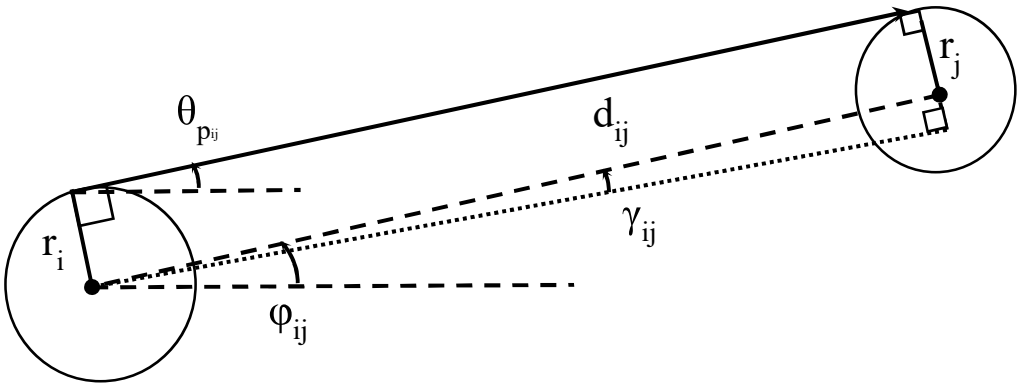

Figure 30. Parameters of Cable Angle Calculations for Multi-Pulley Solution

Cable slopes will be compared with the tangents of the trajectory of point C. The angle of tangent line (θ_{ti}) from point C to nearest pulley can be found as:

$$\theta_{ti} = \text{Atan2}(x_i - x_c; y_i - y_c) + \text{Asin}\left(\frac{r_i}{\sqrt{(x_i - x_c)^2 + (y_i - y_c)^2}}\right) \tag{3.39}$$

where i represents the number of the pulley which is closest to point C. Then, the algorithm for the cable is found as:

$$\text{if } \theta_{t1} > \theta_{p12}$$

$$\theta_t = \theta_{t1}$$

$$\text{elseif } \theta_{t2} > \theta_{p23}$$

$$\theta_t = \theta_{t2}$$

$$\text{else}$$

$$\theta_t = \theta_{t3}$$

The angle θ_t is the active tension angle with respect to coordinate frame x-axis and is used in cable length calculations and force calculations.

3.2.3.4. Closed Loop Cable Drive Design

The cable drive system is optimized such that point C, where cable is attached to the mechanism, follows a path of several straight lines. The four-bar mechanism must be driven in both directions and hence the drive cable is designed to be as a closed-loop system in order to achieve the drive requirements with a single motor. Cable is required to be wrapped around the motor pulley at least one full cycle in order to achieve the desired friction between the pulley and the cable. Other pulleys are intermediate pulleys that are to be designed so that the total theoretical length of the closed-loop cable does not change by large margins. Due to the small variations in the cable length, the cable tension is to be ensured by a simple spring-supported pulley.

The cable length is formulated in sections such as an arc or a tangent line. The formulations change according to the location of the coupler point C.

Tangent line between point C and the i^{th} pulley is:

$$l_{ic} = \sqrt{\left(x_i - x_c\right)^2 + \left(y_i - y_c\right)^2 - r_i^2} \tag{3.40}$$

Tangent line between i^{th} and j^{th} pulleys is:

$$l_{ij} = \sqrt{\left(x_i - x_j\right)^2 + \left(y_i - y_j\right)^2 - \left(r_i - r_j\right)^2} \tag{3.41}$$

The arc-length of the cable wrapped around the j^{th} pulley if point C is in the neighborhood of the pulley:

$$l_{ijc} = r_j \left(\theta_{p_{ij}} - \theta_{p_{jc}}\right) \tag{3.42}$$

The arc-length of the cable wrapped around j^{th} pulley if the cable is connected to other pulleys on both sides, i.e. when point C is not in the neighborhood of the j^{th} pulley:

$$l_{ijk} = r_j \left(\theta_{p_{ij}} - \theta_{p_{jk}}\right) \tag{3.43}$$

The analysis is made in Excel including “if conditioned” formulations. For each pose of the mechanism, the angle of cable is calculated for each pulley and the algorithm represented in Kinematic Analysis Parameters section is applied for comparison. The contact formation and loose of contact is assumed to be smooth between the pulleys and the rope. Pulleys are placed such that the straight line segments

of the path of point C are as close as practically possible to the tangent lines between the pulleys. Locations and radii of the pulleys are determined according to an optimization algorithm run in Excel. The locations and radii of the pulleys from bottom to top in Figure 29, are as follows:

1st pulley: $x_1 = 0$ mm, $y_1 = -150$ mm, $r_1 = 25$ mm.

2nd pulley: $x_2 = 0$ mm, $y_2 = 0$ mm, $r_2 = 65$ mm.

3rd pulley: $x_3 = 85$ mm, $y_3 = 230$ mm, $r_3 = 29$ mm.

4th (motor) pulley: $x_4 = 250$ mm, $y_4 = 340$ mm, $r_4 = 30$ mm.

The total cable length calculated varies between 1339 mm and 1342 mm as shown in Figure 31. This amount of variation is acceptable and can be compensated by either the flexibility of the cable and the pulley joints, or a linear spring attached to the housing of a pulley that ensures that the cable is in tension at all times.

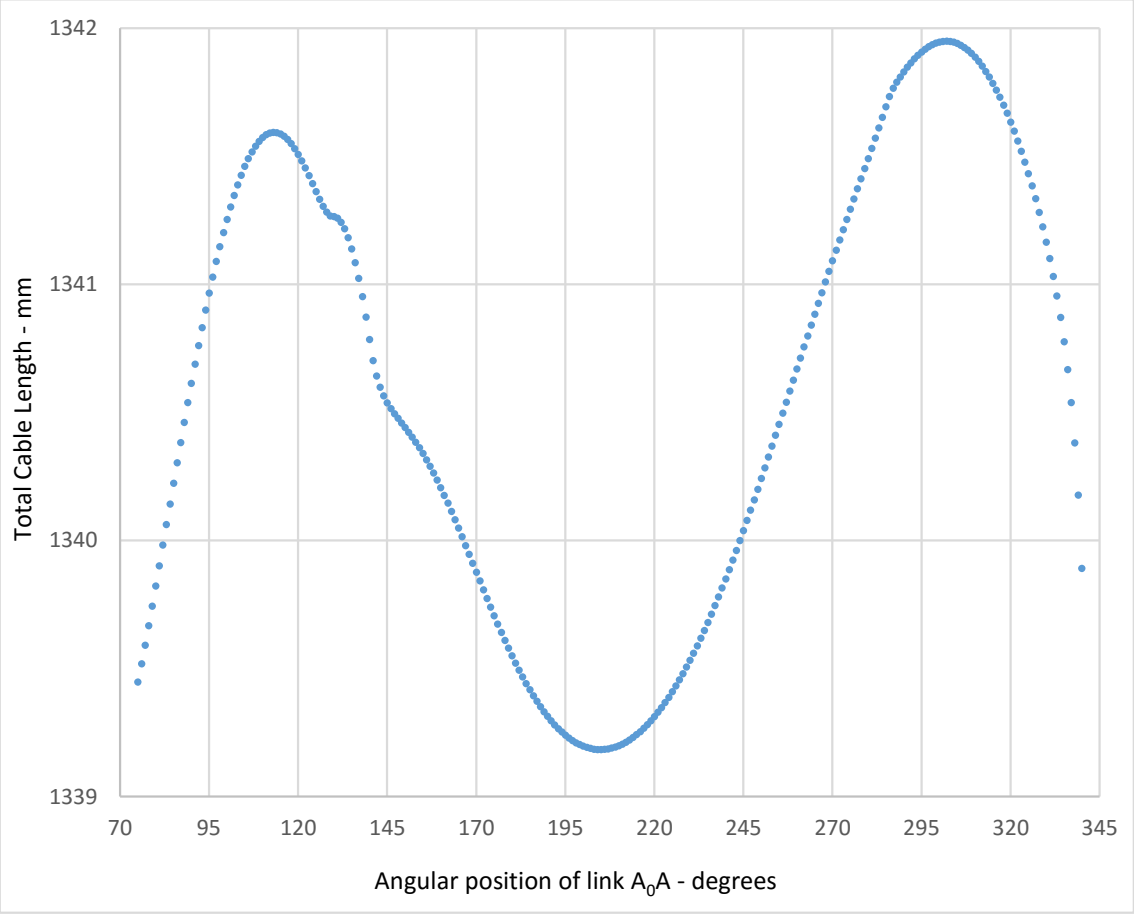

Figure 31. Total Cable Length Variation throughout the Motion

3.2.4. Force Analysis of the Cable Drive System

The exercises are performed with relatively slow speeds, so it is anticipated that the inertial forces are negligible compared to gravitational and external forces. To validate this assumption the accelerations of the joints and centers of gravities of the links are computed for a representative time for the vertical exercise from position 1 to position 2 as 5 s. The 5 s motion corresponds to a speed of 56 mm/s of the cable. Applying the velocity and acceleration analyses, numerical calculations result in maximum angular acceleration of joints to be less than 0.789 rad/s^2 for α_{12}, 0.674 rad/s^2 for α_{13} and 0.077 rad/s^2 for α_{14}. As an example, the maximum acceleration of the center of gravity of the front arm is computed as 278.12 mm/s^2, which is much smaller (2.83%) than the gravitational acceleration 9806.65 mm/s2. Therefore, a static force analysis can be performed instead of a dynamic force analysis.

The static force analysis is performed using the virtual work and free-body-diagram (FBD) methods. Result of both methods are the same as presented in the last part of this subsection.

3.2.4.1. Virtual Work Method for Cable Tension

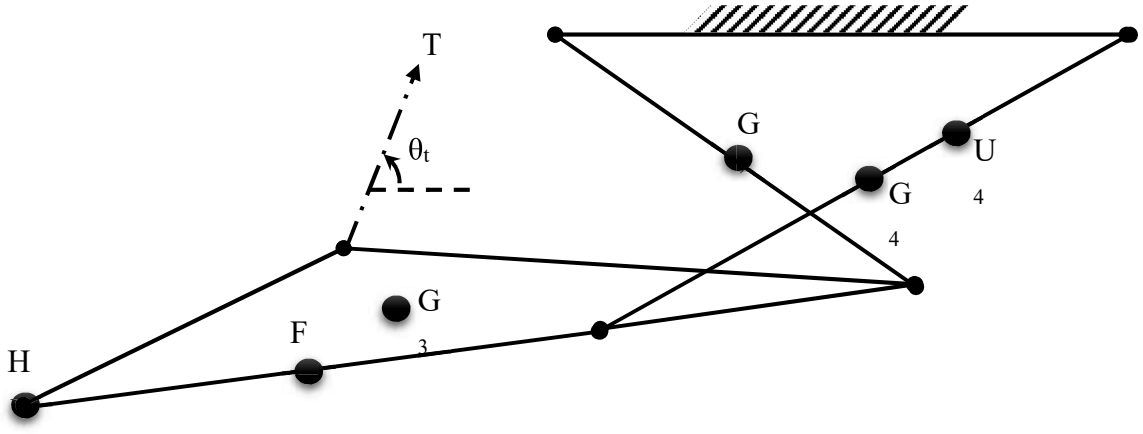

Figure 32. Mass Centers and Location of External Forces

Ignoring all inertial forces as motion is slow, only gravitational forces and cable tension will be applying on mechanism. Figure 32 shows the location of mass centers of all objects in the loop. G_i's are mass centers of links of the four-bar mechanism. G_2 and G_4 are assumed to be at the middle of the links. U_4 is the mass center of upper arm and has a subscript of 4 as it moves together with link 4, which is the rocker. Similarly, F_3 represents the mass center of the forearm and H_3 represents that of the hand. T and θ_t are the magnitude and the angle of the tension force on the cable, respectively. Only the vertical positions for the mass centers are considered as gravitational force does no work in horizontal direction. For point C where tension force T applies, both vertical and horizontal components are needed.

$$G_{2y} = \frac{a_2}{2}\sin\theta_2 \Rightarrow \delta G_{2y} = \frac{a_2}{2}\cos\theta_2\delta\theta_2 \tag{3.44}$$

$$G_{3y} = a_2\sin\theta_2 + \frac{2a_3 + b_3 + h_3}{3}\sin\theta_3 - \frac{c_3}{3}\cos\theta_3 \tag{3.45}$$

$$\Rightarrow \delta G_{3y} = a_2\cos\theta_2\delta\theta_2 + \frac{2a_3 + b_3 + h_3}{3}\cos\theta_3\delta\theta_3 + \frac{c_3}{3}\sin\theta_3\delta\theta_3 \tag{3.46}$$

$$G_{4y} = \frac{a_4}{2}\sin\theta_4 \Rightarrow \delta G_{4y} = \frac{a_4}{2}\cos\theta_4\delta\theta_4 \tag{3.47}$$

$$F_{3y} = a_2\sin\theta_2 + (a_3 + f_3)\sin\theta_3 \Rightarrow \delta F_{3y} = a_2\cos\theta_2\delta\theta_2 + (a_3 + f_3)\cos\theta_3\delta\theta_3 \tag{3.48}$$

$$H_{3y} = a_2\sin\theta_2 + (a_3 + h_3)\sin\theta_3 \Rightarrow \delta H_{3y} = a_2\cos\theta_2\delta\theta_2 + (a_3 + h_3)\cos\theta_3\delta\theta_3 \tag{3.49}$$

$$U_4 = u_4\sin\theta_4 \Rightarrow \delta U_4 = u_4\cos\theta_4\delta\theta_4 \tag{3.50}$$

$$C_x = a_2\cos\theta_2 + (a_3 + b_3)\cos\theta_3 + c_3\sin\theta_3 \tag{3.51}$$

$$\Rightarrow \delta C_x = -a_2\sin\theta_2\delta\theta_2 - (a_3 + b_3)\sin\theta_3\delta\theta_3 + c_3\cos\theta_3\delta\theta_3 \tag{3.52}$$

$$C_y = a_2\sin\theta_2 + (a_3 + b_3)\sin\theta_3 - c_3\cos\theta_3 \tag{3.53}$$

$$\Rightarrow \delta C_y = a_2\cos\theta_2\delta\theta_2 + (a_3 + b_3)\cos\theta_3\delta\theta_3 + c_3\sin\theta_3\delta\theta_3 \tag{3.54}$$

When all equations are divided by $\delta\theta_2$, $\frac{\delta\theta_4}{\delta\theta_2}$ and $\frac{\delta\theta_3}{\delta\theta_2}$ are required to be found. These ratios can be found from the derivative of the loop closure equations:

$$a_2e^{i\theta_2} + a_3e^{i\theta_3} = a_1 + a_4e^{i\theta_4} \Rightarrow i\delta\theta_2a_2e^{i\theta_2} + i\delta\theta_3a_3e^{i\theta_3} = i\delta\theta_4a_4e^{i\theta_4} \tag{3.55}$$

$$-\delta\theta_2a_2\sin\theta_2 = \delta\theta_3a_3\sin\theta_3 - \delta\theta_4a_4\sin\theta_4 \tag{3.56}$$

$$\delta\theta_2a_2\cos\theta_2 = -\delta\theta_3a_3\cos\theta_3 + \delta\theta_4a_4\cos\theta_4 \tag{3.57}$$

$$\begin{pmatrix} \delta\theta_3/\delta\theta_2 \\ \delta\theta_4/\delta\theta_2 \end{pmatrix} = \begin{pmatrix} a_3\sin\theta_3 & -a_4\sin\theta_4 \\ -a_3\cos\theta_3 & a_4\cos\theta_4 \end{pmatrix}^{-1} \begin{pmatrix} -a_2\sin\theta_2 \\ a_2\cos\theta_2 \end{pmatrix} \tag{3.58}$$

$$\frac{\delta\theta_4}{\delta\theta_2} = \frac{a_2\sin(\theta_3-\theta_2)}{a_4\sin(\theta_3-\theta_4)} \tag{3.59}$$

$$\frac{\delta\theta_3}{\delta\theta_2} = \frac{a_2\sin(\theta_4-\theta_2)}{a_3\sin(\theta_3-\theta_4)} \tag{3.60}$$

Then the tension force is computed using the virtual work principle as:

$$T\left(\delta C_x\cos\theta_t + \delta C_y\sin\theta_t\right) = g\left(m_2\delta G_{2y} + m_3\delta G_{3y} + m_4\delta G_{4y} + m_u\delta U_{4y} + m_f\delta F_{3y} + m_h\delta H_{3y}\right) \tag{3.61}$$

$$T = \frac{g\left(m_2\delta G_{2y} + m_3\delta G_{3y} + m_4\delta G_{4y} + m_u\delta U_{4y} + m_f\delta F_{3y} + m_h\delta H_{3y}\right)}{\delta C_x\cos\theta_t + \delta C_y\sin\theta_t} \tag{3.62}$$

3.2.4.2. Calculation of the Cable Tension from the Force Equilibrium Equations

In this method, forces on the links are calculated using the force and moment equilibrium equations using the free-body diagrams (FBDs) (Figure 33-36). As the mechanism is planar, only sum of vertical and horizontal forces and moment sum at one point must be equal to zero. 3 equations can be obtained for each link which makes 9 equations in total for the crank, coupler and rocker links. Unknown parameters are tension the force T and 8 reaction force components for the 4 revolute joints. Sum of vertical and horizontal forces are not calculated for the crank and rocker links as calculating sum of moments on these links on fixed joint centers do not involve the ground reaction forces. So the problem reduces to 5 equations and 5 unknown parameters.

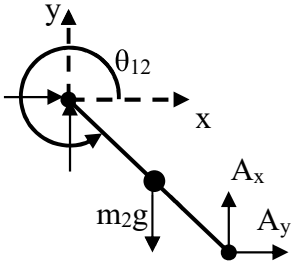

Figure 33. FBD of the Crank Link

For link 2:

$$\sum M_{A_0} = -m_2 g \frac{a_2}{2} \cos\theta_{12} + A_y a_2 \cos\theta_{12} - A_x a_2 \sin\theta_{12} = 0 \tag{3.63}$$

$$A_y = A_x \tan\theta_{12} + \frac{m_2 g}{2} \tag{3.64}$$

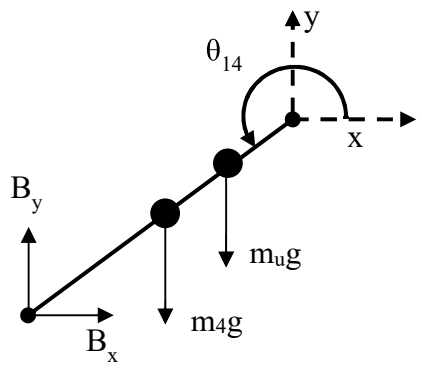

Figure 34. FBD of the Rocker Link

For link 4:

$$\sum M_{B_0} = B_y a_4 \cos\theta_{14} = m_u g u_4 \cos\theta_{14} + m_4 g \frac{a_4}{2} \cos\theta_{14} + B_x a_2 \sin\theta_{14} = 0 \tag{3.65}$$

$$B_y = B_x \tan\theta_{14} + \frac{m_4 g}{2} + m_u g \frac{u_4}{a_4} \tag{3.66}$$

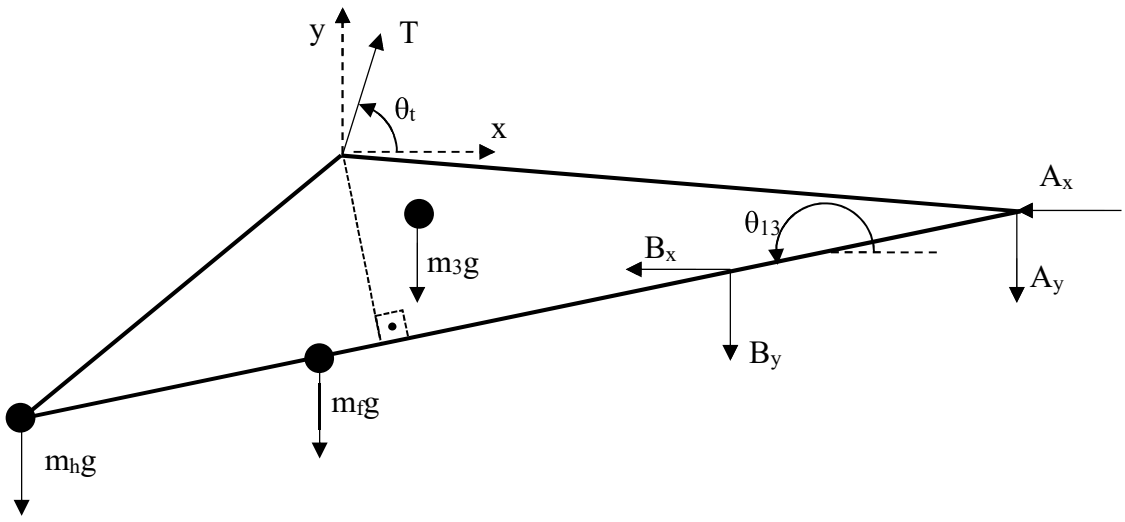

Figure 35. FBD of the Coupler Link

Force equilibrium for link 3:

$$\sum F_x = T\cos\theta_t - A_x - B_x = 0 \Rightarrow T = \frac{A_x + B_x}{\cos\theta_t} \tag{3.67}$$

$$\sum F_y = T\sin(\theta_t) - A_y - B_y - m_3 g - m_f g - m_h g = 0 \tag{3.68}$$

$$A_y + B_y = -m_3 g - m_f g - m_h g + T\sin\theta_t = -m_3 g - m_f g - m_h g + \frac{A_x + B_x}{\cos\theta_t}\sin(\theta_t) \tag{3.69}$$

Using the A_y and B_y expressions found for links 2 and 4 and equating with the $A_y + B_y$ expression found for link 3:

$$A_y + B_y = A_x \tan\theta_{12} + \frac{m_2 g}{2} + B_x \tan\theta_{14} + m_u g\frac{u_4}{a_4} + \frac{m_4 g}{2} \tag{3.70}$$

$$-m_3 g - m_f g - m_h g + (A_x + B_x)\tan\theta_t = A_x \tan\theta_{12} + \frac{m_2 g}{2} + B_x \tan\theta_{14} + m_u g\frac{u_4}{a_4} + \frac{m_4 g}{2} \tag{3.71}$$

$$D_{11}A_x + D_{12}B_x = R_1 \tag{3.72}$$

where

$$D_{11} = \tan\theta_t - \tan\theta_{12} \tag{3.73}$$

$$D_{12} = \tan\theta_t - \tan\theta_{14} \tag{3.74}$$

$$R_1 = \left(m_3 + m_f + m_h + \frac{m_2}{2} + m_u\frac{u_4}{a_4} + \frac{m_4}{2}\right)g \tag{3.75}$$

Moment equilibrium for link 3:

$$\sum M_C = M_{C/A} + M_{C/B} + M_{C/G_3} + M_{C/F} + M_{C/H} = 0 \tag{3.76}$$

$$M_{C/A} = \left(c_3\cos(\theta_{13}) - (a_3 + b_3)\sin(\theta_{13})\right)A_x + \left(c_3\sin(\theta_{13}) + (a_3 + b_3)\cos(\theta_{13})\right)A_y \tag{3.77}$$

$$M_{C/B} = \left(c_3\cos(\theta_{13}) - b_3\sin(\theta_{13})\right)B_x + \left(c_3\sin(\theta_{13}) + b_3\cos(\theta_{13})\right)B_y \tag{3.78}$$

$$M_{C/G_3} = m_3 g\left(\frac{2}{3}c_3\sin(\theta_{13}) + \frac{a_3 + 2b_3 - h_3}{3}\cos(\theta_{13})\right) \tag{3.79}$$

$$M_{C/F} = m_f g\left(c_3\sin(\theta_{13}) - (f_3 - b_3)\cos(\theta_{13})\right) \tag{3.80}$$

$$M_{C/H} = m_h g\left(c_3\sin(\theta_{13}) - (h_3 - b_3)\cos(\theta_{13})\right) \tag{3.81}$$

$$D_{21}A_x + D_{22}B_x = R_2 \tag{3.82}$$

where

$$D_{21} = -c_3\cos(\theta_{13}) + (a_3 + b_3)\sin(\theta_{13}) - \left(c_3\sin(\theta_{13}) + (a_3 + b_3)\cos(\theta_{13})\right)\tan(\theta_{12}) \tag{3.83}$$

$$D_{22} = -c_3\cos(\theta_{13}) + b_3\sin(\theta_{13}) - \left(c_3\sin(\theta_{13}) + b_3\cos(\theta_{13})\right)\tan(\theta_{14}) \tag{3.84}$$

$$R_2 = \left(\left(c_3\sin(\theta_{13}) + (b_3)\cos(\theta_{13})\right)\left(\frac{m_2 + m_4}{2} + \frac{m_u u_4}{a_4}\right) + \frac{m_2}{2}a_3\cos(\theta_{13})\right)g + M_{C/G_3} + M_{C/F} + M_{C/H} \tag{3.85}$$

The two linear equations in A_x and A_y can be written in matrix form and solved as

$$\begin{pmatrix} D_{11} & D_{12} \\ D_{21} & D_{22} \end{pmatrix} \begin{pmatrix} A_x \\ B_x \end{pmatrix} = \begin{pmatrix} R_1 \\ R_2 \end{pmatrix} \tag{3.86}$$

$$\Delta = D_{11}D_{22} - D_{12}D_{21} \tag{3.87}$$

$$A_x = \frac{R_1 D_{22} - R_2 D_{12}}{\Delta} \tag{3.88}$$

$$B_x = \frac{R_2 D_{11} - R_1 D_{21}}{\Delta} \tag{3.89}$$

Then the tension force is found as

$$T = \frac{A_x + B_x}{\cos\theta_t} \tag{3.90}$$

The tension force obtained herein is equivalent to the one found using the virtual work method.

3.2.4.3. Numerical Calculations

The force analysis formulations obtained in the previous sections are implemented in Excel® for numerical calculations. Scaled link lengths are a_1 = 295.2 mm, a_2 = 191.9 mm, a_3 = 202.1 mm, b_3 = 25.5 mm, c_3 = -27 mm, f_3 = 142.0 mm (mass center distance of the front arm from the elbow), h_3 = 375.9 mm (mass center distance of the hand from the elbow), u_4 = 143.9 mm (mass center distance of the upper arm from the shoulder center) and a_4 = 330.1 mm. Mass of links and body parts are m_2 = 0.230 kg (crank mass), m_3 = 0.693 kg (coupler mass), m_4 = 0.396 kg (rocker mass), m_u = 3.25 kg (upper arm mass), m_f = 1.87 kg (front arm mass) and m_h = 0.65 kg (hand mass).

Cable actuation analysis resulted in a maximum of 80 N tension force for motion in vertical plane and approximately 25.5 N of maximum tension force for the motion in the oblique plane. Actuator pulley radius is selected as 30 mm so that the rope is wrapped around the pulley no more than three full cycles. Therefore, a motor with 2.5 N·m maximum torque is sufficient for the actuation (Figure 36-Figure 39).

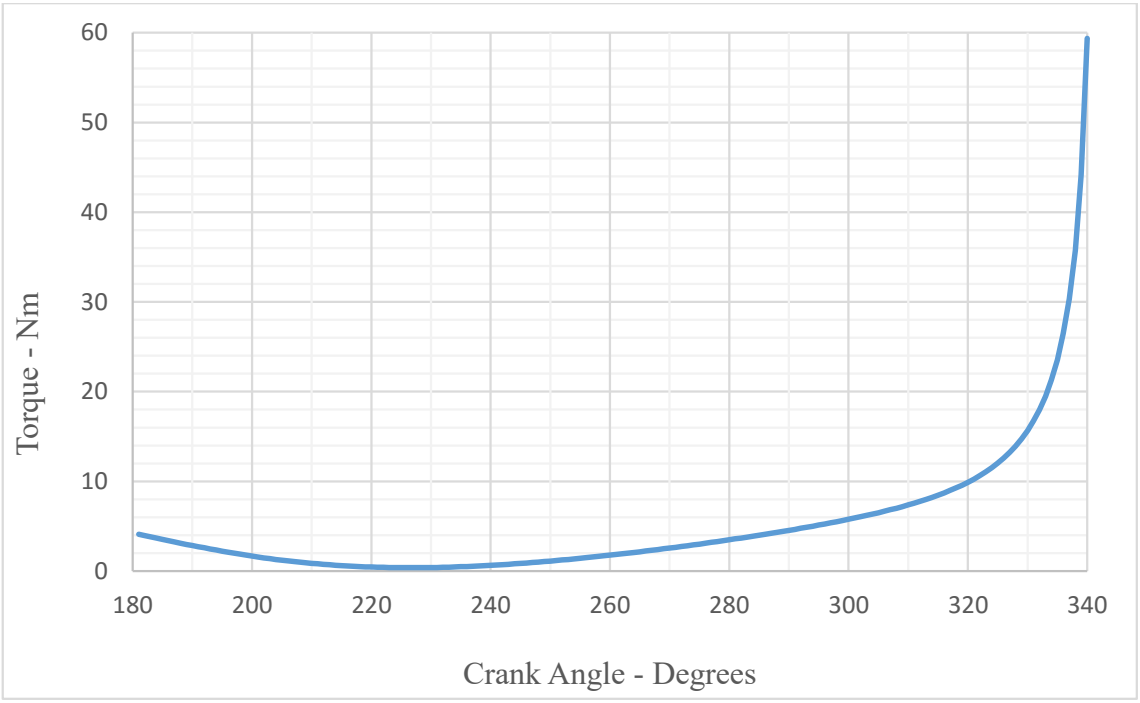

Figure 36. Motor Torque for Crank Actuation in Vertical Plane

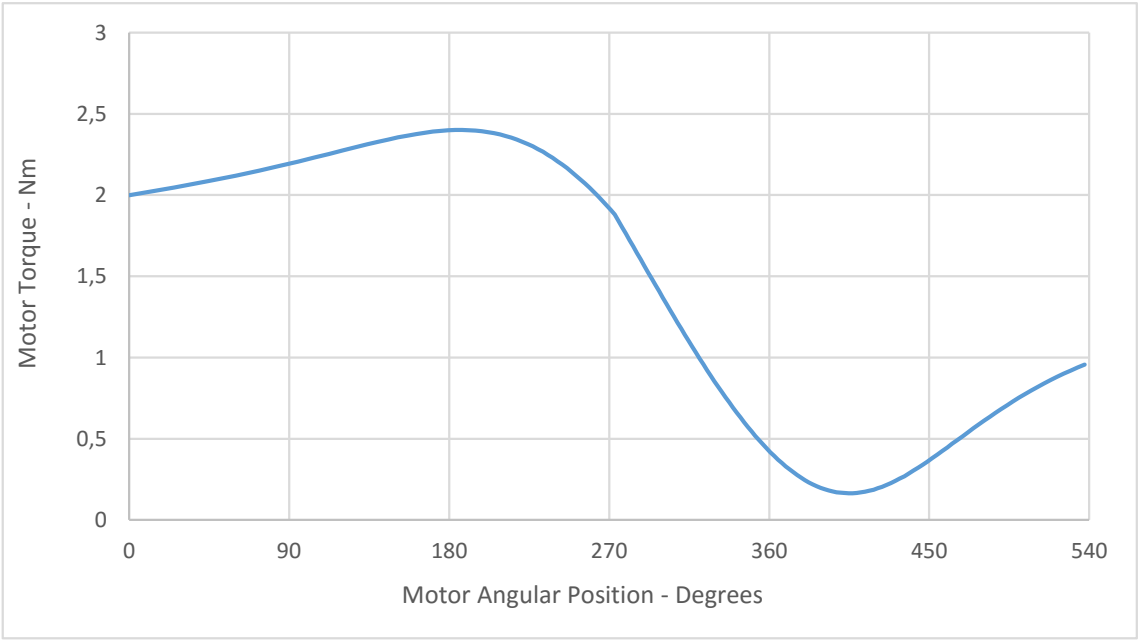

Figure 37. Motor Torque for Cable Actuation in Vertical Plane

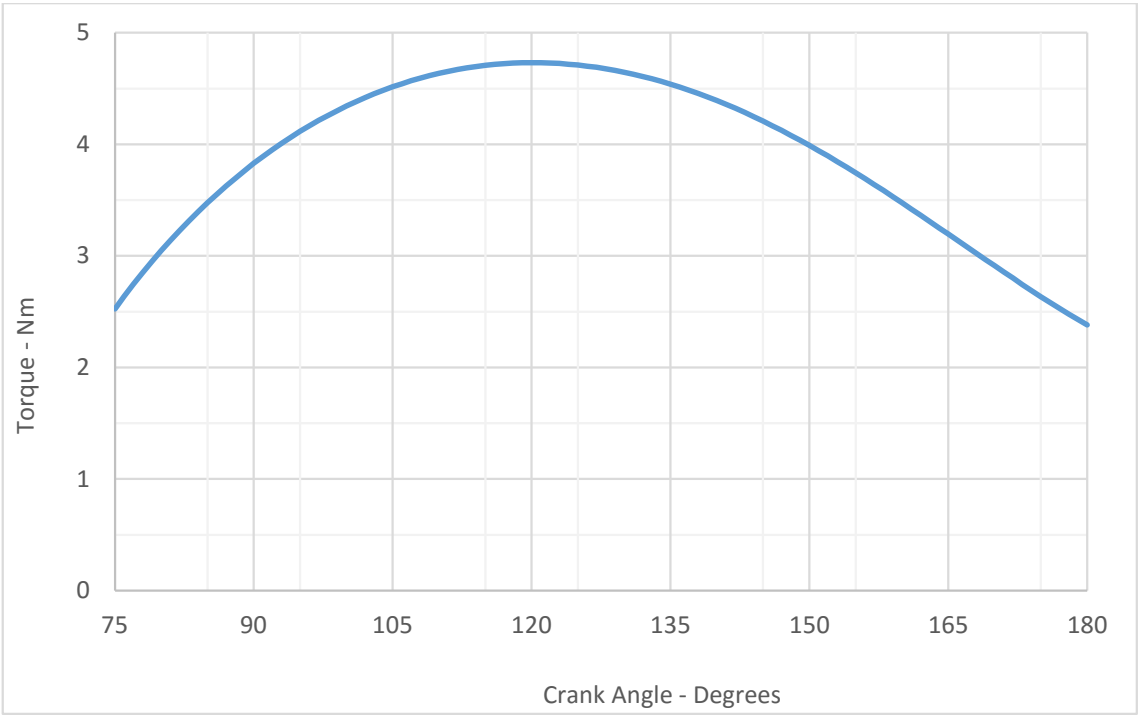

Figure 38. Motor Torque for Crank Actuation in Oblique Plane

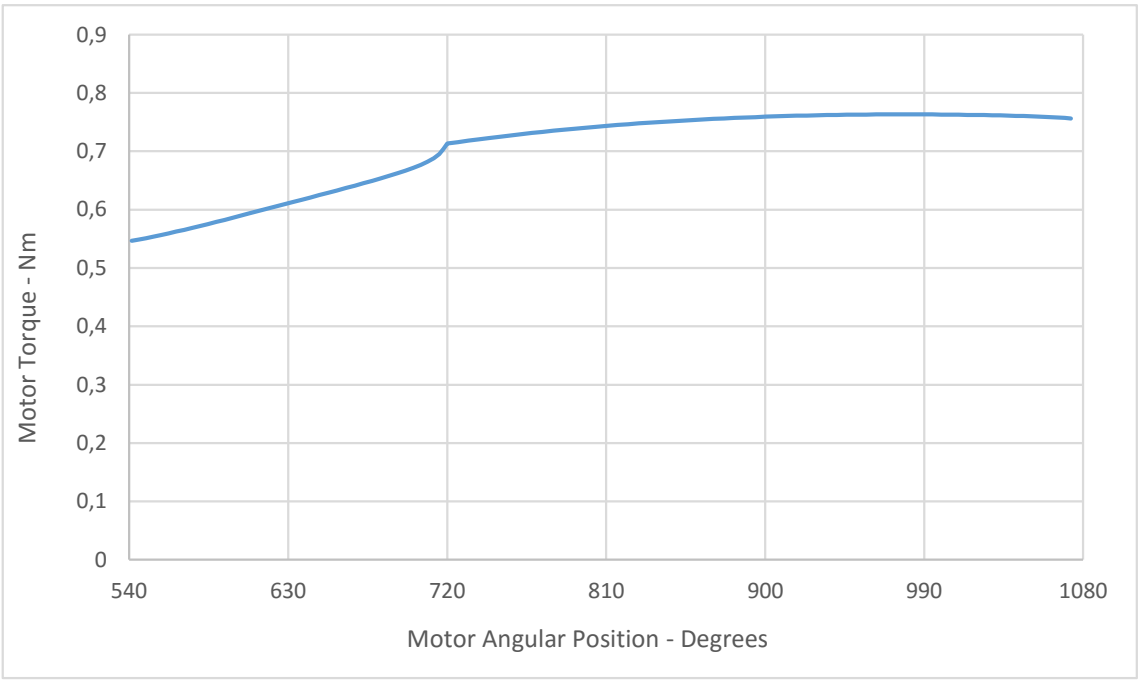

Figure 39. Motor Torque for Cable Actuation in Oblique Plane

CHAPTER 4

THE PROTOTYPE

The parts and the assembly of the prototype of the final design are presented in this Chapter. Manufactured parts of the system is presented as views from the CAD models. The technical drawings are presented in Appendix A.

4.1. Sub-Systems

The designed system is composed of 4 sub-systems: the fixed base, the mechanism frame, the linkage and the actuation system.

4.1.1. The Base

The main design criteria of the base are supporting the load on the system and to provide the kinematic element for re-orientation of the mechanism frame. Base parts must not interfere with the patient while the system works. The system is desired to be placed on the corner of a wall. Hence, the support is designed to lean on the wall on which it will be fixed (Figure 40). Base part is made of steel profiles. Parts are cut with necessary angles. Bottom parts of the base are cut in 45° and welded together. Top parts of the base are cut as detailed in technical drawings in Appendix A. Purpose of bottom parts is only to support vertical element of base. Upper parts of the base are cut in specific angles such that the central axis of the kinematic element of the re-orientation joint on the base comes into right orientation. The right orientation for the kinematic element is such that the bottom of the frame is parallel to ground when the plane of motion of the mechanism is perpendicular to the wall at the back. After the system is manufactured, the plane of motion of the mechanism is measured to be slightly different than being perpendicular to back wall. This constructional error is overcome by placing patient seat accordingly.

a) 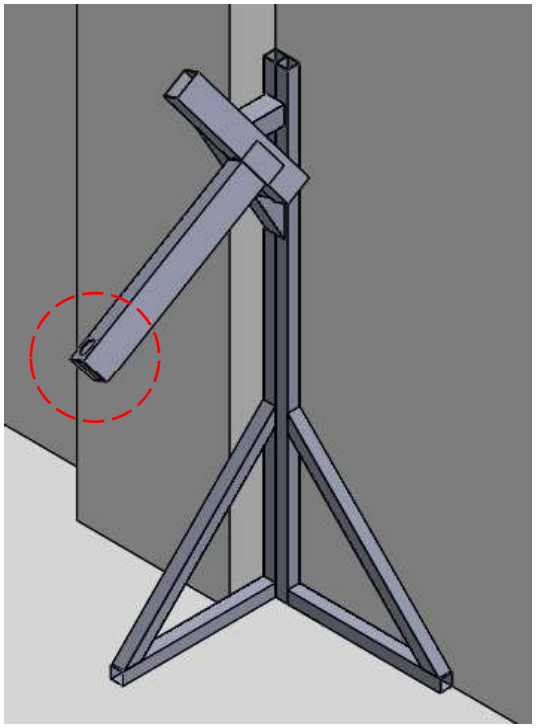 b) 

Figure 40. The Base Design: a) the CAD Model and b) the Manufactured Base

The kinematic element of the base is marked with dashed line circle in Figure 40. Two bearings for the re-orientation joint are embedded in a hard plastic housing. Details are shown in . The iron profile is intentionally made transparent.

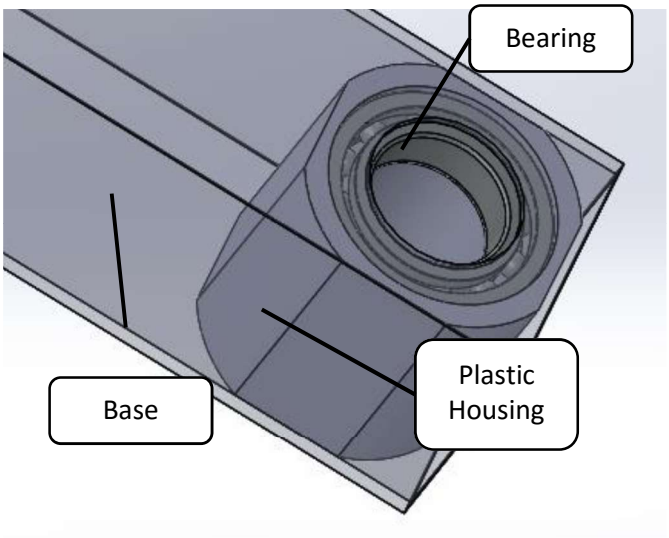

Figure 41. Kinematic Element Design on the Base

4.1.2. The Mechanism Frame

The frame is one of the most critical parts of the mechanism. Moving links and cable actuation elements are placed on the mechanism frame. In addition, the frame should have a kinematic element that will make the re-orientation joint with the base.

First stage of the design did not contain cable actuation and therefore the design of the connection between the base and the mechanism frame was as shown in Figure 42. The cylindrical part of the mechanism frame is the kinematic element of the re-orientation joint. The full prototype of the old design is not manufactured. The base and the three moving links of the four bar mechanism is intentionally made transparent in the figure.

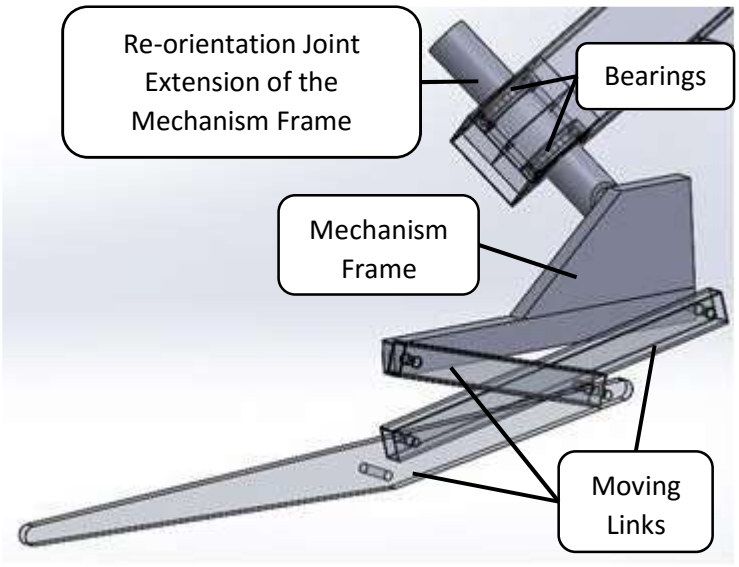

Figure 42. The Mechanism Frame Design before Cable Actuation

Cable actuation requires two intermediate pulleys and a motor pulley. Modified frame (Figure 43) includes kinematic elements (holes) for revolute joints with intermediate pulleys and support for motor pulley and motor attachment. Frame is completely made of aluminum. Straight sections are cut from aluminum material of rectangular cross-section of 30 mm by 20 mm with a wall thickness of 2 mm. Rectangular profile parts are screwed to aluminum sheets of 3 mm thickness. Then, the holes are drilled on both sheet and profile parts. Cylindrical part for the re-orientation

joint is also screwed directly and through small additional corner parts to the rest of the frame. The large hollow cylindrical plastic part on the top is the motor pulley housing which will be mentioned once more in the actuation elements part.

a) 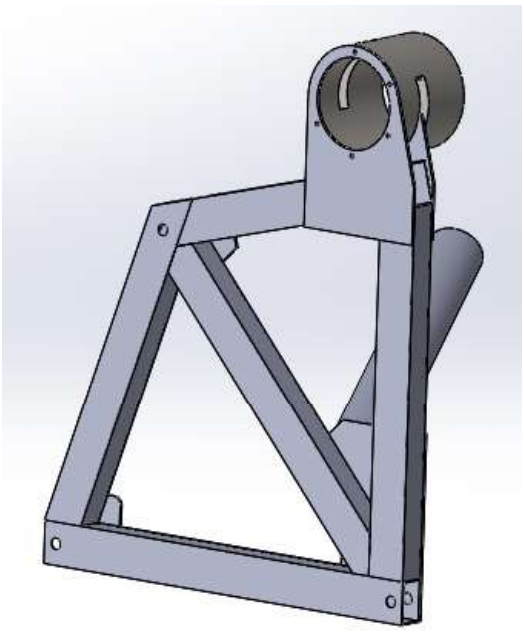 b) 

Figure 43. The Modified Mechanism Frame: a) the CAD Model and b) the Manufactured Model

4.1.3. The Linkage

Links are manufactured from Aluminum rectangular profiles or thick sheets. Aluminum is preferred for the moving links in order to have lighter weight. The crank needs to have only two kinematic elements to connect to the mechanism frame and the coupler link. The rocker has two kinematic elements, connecting to the mechanism frame and the coupler link, and will have a compliant attachment to the upper arm which is not shown in Figure 44. Upper arm may need to move relatively to the rocker as the link length may not exactly match the humerus bone length, which causes ergonomic problems. Hence, small longitudinal motion may be necessary for the patient's comfort. Therefore, connection of the upper arm is not designed to be rigid. Finally, the coupler link (Figure 45) needs to have two kinematic elements, connecting

to the crank and the rocker, a cable connection extension and some space to support the forearm.

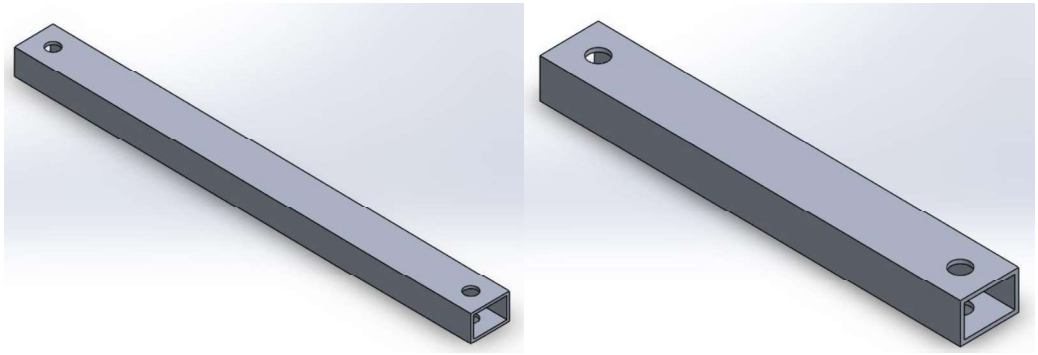

Figure 44. Rocker Link (Left) and Crank Link (Right)

a)

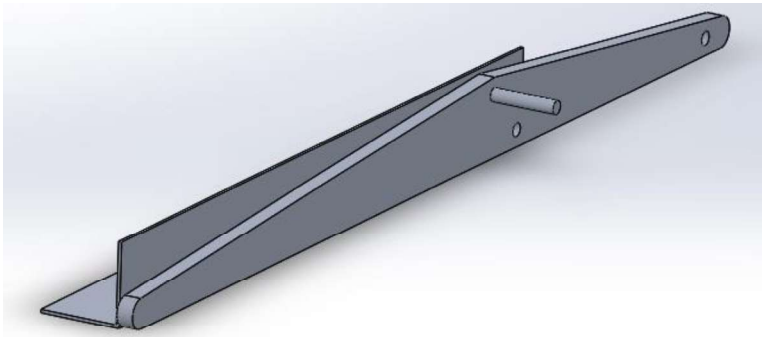

b)

Figure 45. a) The Coupler Link and b) the manufactured mechanism

4.1.4. The Actuation Elements

Cable is designed to be a closed loop chain. Both ends are attached to point C on the coupler, cable is wrapped around the intermediate pulleys and the motor pulley.

Friction between the pulley and the cable is desired only for motor pulley (Figure 46). Therefore, cable is wrapped around the motor pulley more than one full revolution. As the cable is not desired to be wrapped around itself, the motor pulley is designed to have a helical groove. The motor pulley must make axial translation as it rotates in order to let the cable follow the helical thread while it is wrapped. Therefore the connection of the motor pulley to the motor shaft allows relative translation and the pulley makes a screw motion with respect to the casing. The motor pulley is manufactured from easy-to-handle hard plastic material.

a) 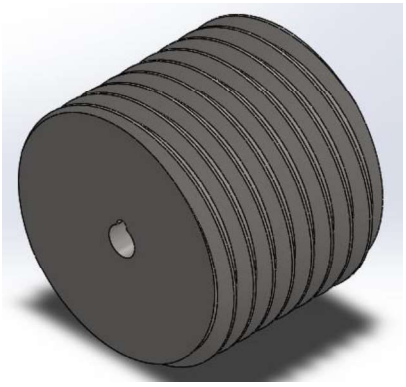 b) 

Figure 46. Motor Pulley: a) the CAD Model and b) the Manufactured Model

The motor pulley casing (Figure 47) has a small cut part in order not to interfere with the cable. The casing is attached on the mechanism frame (Figure 43), while the motor is attached on the other side of the casing and the motor pulley moves inside it.

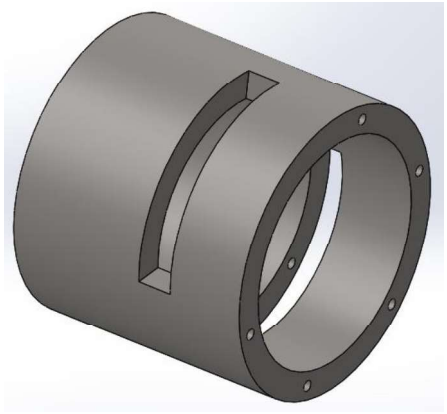

Figure 47. The CAD Model of Motor Pulley Casing

Finally, an assembly of all actuation elements assembled is shown in Figure 48.

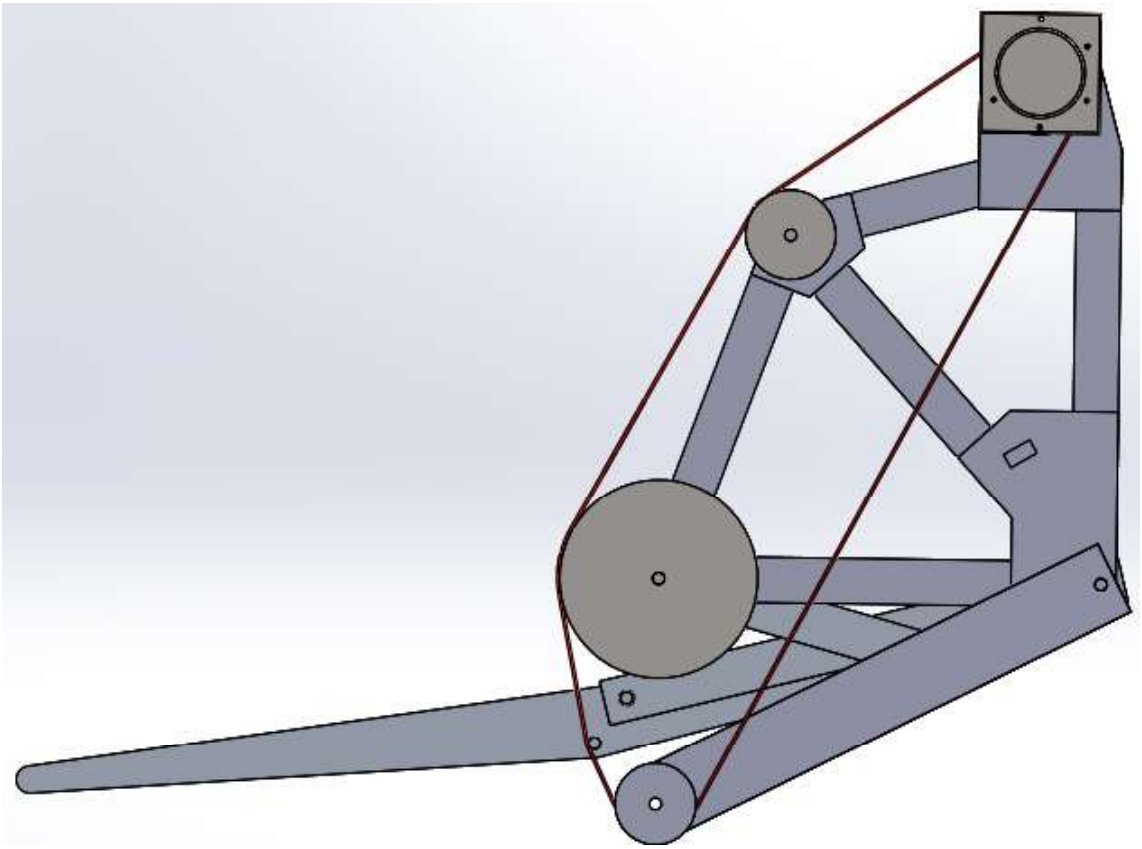

Figure 48. The CAD Model of Final Assembly of Elements

4.1.5. Actuator

According to analysis in Chapter 3, a motor with maximum torque of 2.5 Nm calculated to be enough for the actuation. Maximum motor speed requirement is calculated as 8.26 rev/min. A step motor that meets the requirements was used due to availability. The 2-phase stepper motor is Vexta brand model PK2913-E4.0A and has 1.8° step size. Motor speed-torque characteristics are given in Figure 49. The stepper motor is driven through the micro-step driver 2H504 and Arduino Uno.

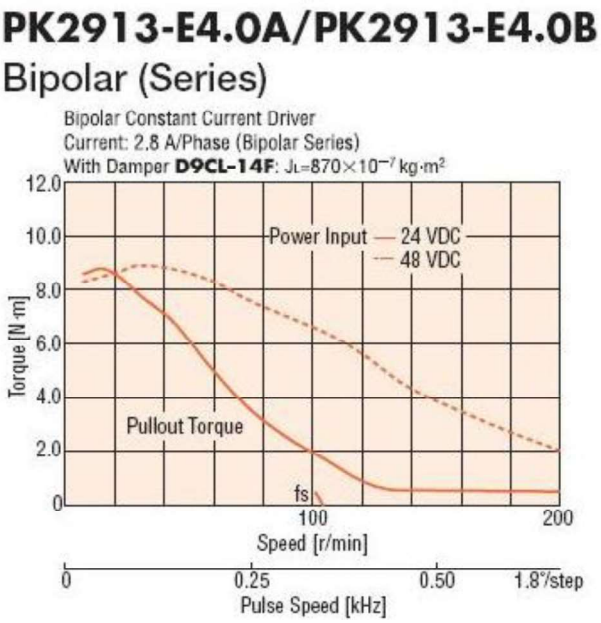

Figure 49. Stepper Motor Characteristics [39]

4.2. Tests

The system is not tested with motor drive as the step motor is driven with position control and there is no torque measuring element for the motor. In order to measure the torque on the motor pulley, static balance torque is determined for specific poses for the motion in vertical plane. Human arm is attached to links with wrist splint and hook & loop tapes as shown in Figure 50.

Figure 50. Attachment of the Human Arm to the System

A hard plastic pin is inserted in the motor pulley instead of motor shaft and a long bolt is joined perpendicular to the plastic pin. A hand scale of 10^{-2} kgf sensitivity is attached at the tip of 100 mm long bolt (Figure 51). As the force measured on hand scale is in kgf, experimental torque value is calculated as:

$$T_{experimental} = F_{measured} \cdot 9.81 \frac{m}{s^2} \cdot 0.1 \text{ m} \quad (4.1)$$

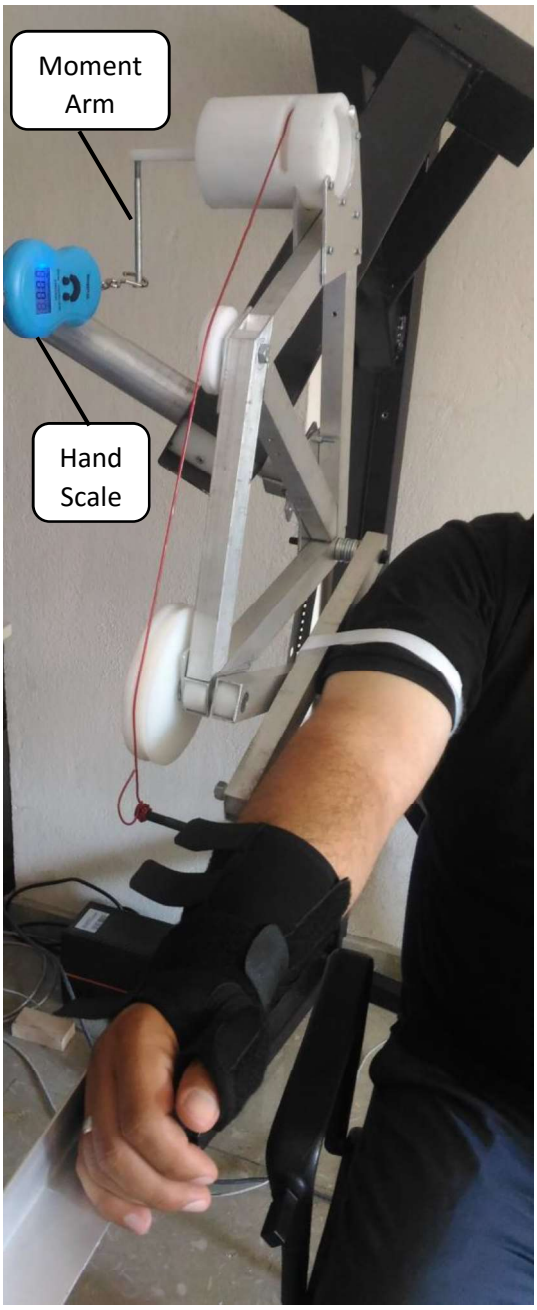

Figure 51. Experimental Setup for Torque Measurements

The measured torque values are compared with the expected torques in Figure 52.

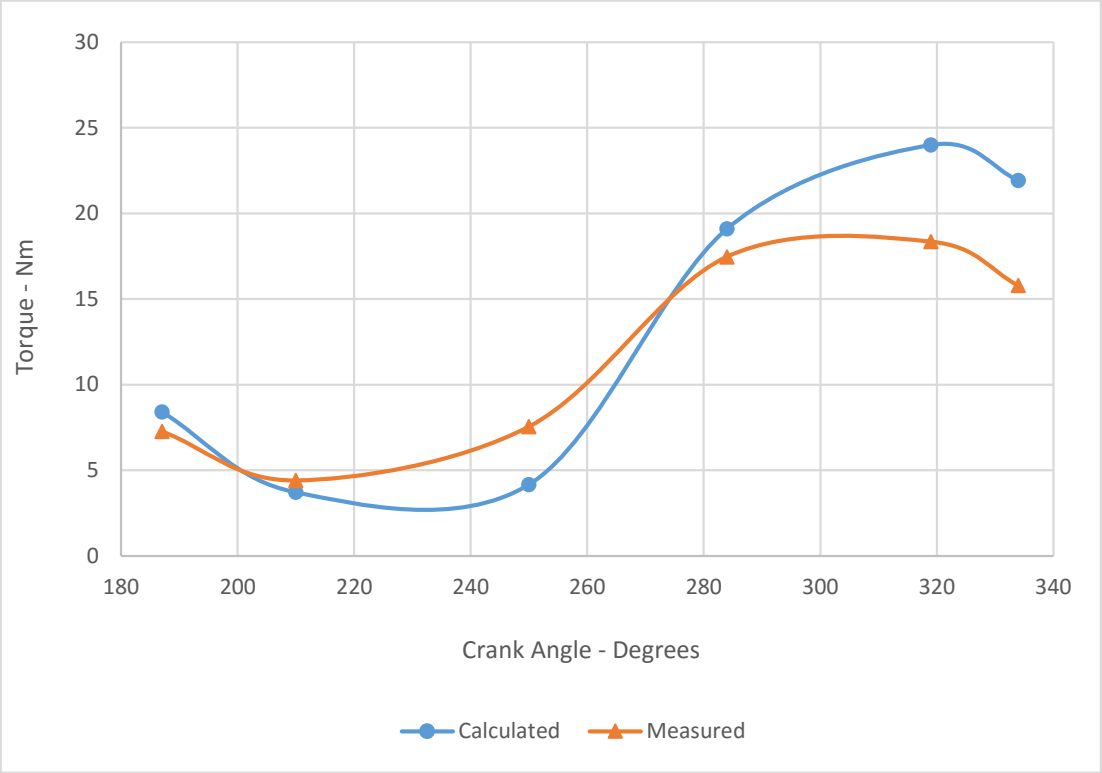

Figure 52. Measured Torque Results Compared to Calculated Torques

The rise and fall of the force measurements through the motion is similar to the calculated values. The difference may arose from a number of reasons. First, the orientation of the bottom of the mechanism frame is not parallel to the ground due to some constructional problems. The angular error is measured as 4.7°. The direction of gravity on mechanism changes and the balance of the forces change for all poses.

Another reason that may have caused the difference is that the real arm mass of subject may not have matched the calculated arm mass. Besides, the center of gravity may not be at or may slip from the location where it is assumed to be. Still, the measurements match the expected static force variance through the path.

CHAPTER 5

CONCLUSION

A single dof mechanism is designed to support two motions of rehabilitation of the human arm. The mechanism design is modelled as a three-position synthesis problem with additional constraints. The first designed mechanism met the motion requirements but had actuation problems. An extra dyad solution is introduced to overcome this problem. However, this solution caused problems of back-drivability. Then, cable actuation solution is introduced which reduced motor torque demand to 2.4 Nm.

A re-orientable support is designed for the prototype. The mechanism frame is modified to include the kinematic elements for the re-orientation joint and the intermediate pulleys. The motor pulley is designed to have helical grooves so that the cable is never wrapped on itself. The connection between the motor pulley and the motor shaft, also motor pulley casing is designed such that the pulley makes screw motion while being actuated by the rotary motor. The coupler link is modified with an extension on the side in order to support the forearm better.

Mechanism does not have height adjustment as the idea is to design the system specifically for a patient. The link lengths are also non-adjustable as they will be built based on length of the patient's humerus bone.

The test results show that the mechanism works even with flaws in construction. As a future work, a more precise testing procedure that supply continuous data through the motion should be applied when testing with patients.

In addition, the actuation can be further developed as a future study. The actuation system may be developed with feedback control in order to achieve semi-supportive or resistive mode in the actuation.

REFERENCES

1. Langhorne, P., J. Bernhardt and G. Kwakkel, Stroke rehabilitation. The Lancet, 2011. 377(9778): p. 1693-1702.

2. Schaechter, J.D., Motor rehabilitation and brain plasticity after hemiparetic stroke. Progress in Neurobiology, 2004. 73(1): p. 61-72.

3. Adebiyi, D.A., Fabrication and characterization of beta-prototype MIT Manus : an intelligent machine for upper-limb physical therapy. 1998.

4. Casadio, M., V. Sanguineti, P.G. Morasso and V. Arrichiello, Braccio di Ferro: a new haptic workstation for neuromotor rehabilitation. Technol Health Care, 2006. 14(3): p. 123-42.

5. Pons, J.L., Rehabilitation exoskeletal robotics. The promise of an emerging field. IEEE Eng Med Biol Mag, 2010. 29(3): p. 57-63.

6. Hogan, N., H.I. Krebs, J. Charnnarong, P. Srikrishna and A. Sharon. MIT-MANUS: a workstation for manual therapy and training. I. in Robot and Human Communication, 1992. Proceedings., IEEE International Workshop on. 1992.

7. Reinkensmeyer, D.J., J.P. Dewald and W.Z. Rymer, Guidance-based quantification of arm impairment following brain injury: a pilot study. IEEE Trans Rehabil Eng, 1999. 7(1): p. 1-11.

8. Sheng, B., Y. Zhang, W. Meng, C. Deng and S. Xie, Bilateral robots for upper-limb stroke rehabilitation: State of the art and future prospects. Med Eng Phys, 2016.

9. Xydas, E., A. Mueller and L.S. Louca, Minimally Actuated Four-Bar Linkages for Upper Limb Rehabilitation. MESROB 2016, 2016. 5th International Workshop on Medical and Service Robots.

10. Health Risks Associated with being a physical therapist or physical therapist assistant student. http://www.canton.edu/sci_health/pta/pdf/Health_Risks.pdf.

11. Lo, H.S. and S.Q. Xie, Exoskeleton robots for upper-limb rehabilitation: State of the art and future prospects. Medical Engineering & Physics, 2012. 34(3): p. 261-268.

12. Lo , A.C., P.D. Guarino , L.G. Richards , J.K. Haselkorn , G.F. Wittenberg , D.G. Federman , R.J. Ringer , T.H. Wagner , H.I. Krebs , B.T. Volpe , C.T.J. Bever , D.M. Bravata , P.W. Duncan , B.H. Corn , A.D. Maffucci , S.E. Nadeau , S.S. Conroy , J.M. Powell , G.D. Huang and P. Peduzzi Robot-Assisted Therapy for Long-Term Upper-Limb Impairment after Stroke. New England Journal of Medicine, 2010. 362(19): p. 1772-1783.

13. Eraz, T., S. Coşkun, Y. Gökmen and M.C. Dede, Omuz için Tek Serbestlik Dereceli Fizik Tedavi Sistemi Tasarımı ve En İyileştirmesi. Otomatik Kontrol Ulusal Toplantısı, TOK 2014, 2014.

14. Nunes, W.M., L.A.O. Rodrigues, L.P. Oliveira, J.F. Ribeiro, J.C.M. Carvalho, R.S. Gon, x00E and alves. Cable-based parallel manipulator for rehabilitation of shoulder and elbow movements. in 2011 IEEE International Conference on Rehabilitation Robotics. 2011.

15. Gezgin, E., Biokinematic analysis of human arm. 2006: p. 44-48.

16. Jackson, A.E., R.J. Holt, P.R. Culmer, S.G. Makower, M.C. Levesley, R.C. Richardson, J.A. Cozens, M.M. Williams and B.B. Bhakta, Dual robot system for upper after stroke: the design limb rehabilitation process. Proceedings of the Institution of Mechanical Engineers Part C-Journal of Mechanical Engineering Science, 2007. 221(7): p. 845-857.

17. Gopura, R.A.R.C., D.S.V. Bandara, K. Kiguchi and G.K.I. Mann, Developments in hardware systems of active upper-limb exoskeleton robots: A review. Robotics and Autonomous Systems, 2016. 75, Part B: p. 203-220.

18. Nef, T. and R. Riener, ARMin - Design of a novel arm rehabilitation robot. 2005 Ieee 9th International Conference on Rehabilitation Robotics, 2005: p. 57-60.

19. Nef, T., M. Guidali and R. Riener, ARMin III – arm therapy exoskeleton with an ergonomic shoulder actuation. Applied Bionics and Biomechanics, 2009. 6(2): p. 127-142.

20. Brackbill, E.A., Y. Mao, S.K. Agrawal, M. Annapragada and V.N. Dubey, Dynamics and Control of a 4-dof Wearable Cable-driven Upper Arm Exoskeleton. Icra: 2009 Ieee International Conference on Robotics and Automation, Vols 1-7, 2009: p. 2308-2313.

21. Agrawal, S.K., V.N. Dubey, J.J. Gangloff, E. Brackbill, Y. Mao and V. Sangwan, Design and Optimization of a Cable Driven Upper Arm Exoskeleton. Journal of Medical Devices-Transactions of the Asme, 2009. 3(3): p. 031004.

22. Mao, Y. and S.K. Agrawal, Wearable Cable-driven Upper Arm Exoskeleton - Motion with Transmitted Joint Force and Moment Minimization. 2010 Ieee International Conference on Robotics and Automation (Icra), 2010: p. 4334-4339.

23. Mao, Y. and S.K. Agrawal, A Cable Driven Upper Arm Exoskeleton for Upper Extremity Rehabilitation. 2011 Ieee International Conference on Robotics and Automation (Icra), 2011.

24. Mao, Y. and S.K. Agrawal, Design of a Cable-Driven Arm Exoskeleton (CAREX) for Neural Rehabilitation. Ieee Transactions on Robotics, 2012. 28(4): p. 922-931.

25. Mao, Y. and S.K. Agrawal, Transition from Mechanical Arm to Human Arm with CAREX: a Cable Driven ARm EXoskeleton (CAREX) for Neural Rehabilitation. 2012 Ieee International Conference on Robotics and Automation (Icra), 2012: p. 2457-2462.

26. Mao, Y., X. Jin and S.K. Agrawal, Real-Time Estimation of Glenohumeral Joint Rotation Center With Cable-Driven Arm Exoskeleton (CAREX)-A Cable-Based Arm Exoskeleton. J Mech Robot, 2014. 6(1): p. 0145021-145025.

27. Ball, S.J., I.E. Brown and S.H. Scott, A planar 3DOF robotic exoskeleton for rehabilitation and assessment. Conf Proc IEEE Eng Med Biol Soc, 2007. 2007: p. 4024-7.

28. Garrec, P., J.P. Martins, F. Gravez, Y. Measson and Y. Perrot, A New Force-Feedback, Morphologically Inspired Portable Exoskeleton. The 15th IEEE International Symposium on Robot and Human Interactive Communication, 2006.

29. Garrec, P., J.P. Friconneau, Y. Measson and Y. Perrot, ABLE, an Innovative Transparent Exoskeleton for the Upper-Limb. 2008 Ieee/Rsj International Conference on Robots and Intelligent Systems, Vols 1-3, Conference Proceedings, 2008: p. 1483-1488.

30. Jarrasse, N., J. Robertson, P. Garrec, J. Paik, V. Pasqui, Y. Perrot, A. Roby-Brami, D. Wang and G. Morel, Design and acceptability assessment of a new reversible orthosis. 2008 Ieee/Rsj International Conference on Robots and Intelligent Systems, Vols 1-3, Conference Proceedings, 2008: p. 1933-1939.

31. Garrec, P., Design Of An Anthropomorphic Upper Limb Exoskeleton Actuated By Ball-Screws And Cables. U.P.B. Sci. Bull., Series D, 2010. 72(2).

32. Papadopoulos, E. and G. Patsianis, Design of an exoskeleton mechanism for the shoulder joint. Proc. Twelfth World Congr. in Mechanism and Machine Sci., Besancon, France, 2007: p. 1-6.

33. Galiana, I., F.L. Hammond, R.D. Howe and M.B. Popovic. Wearable soft robotic device for post-stroke shoulder rehabilitation: Identifying misalignments. in 2012 IEEE/RSJ International Conference on Intelligent Robots and Systems. 2012.

34. Sandor, G.N. and A.G. Erdman, Advanced Mechanism Design, vol. I and II Prentice-Hall Inc, 1984.

35. Sağır, M., Uzun kemik radyografilerinden boy hesaplama formüllerinin oluşturulması. M.Sc. Thesis, 1994.

36. Plagenhoef, S., F.G. Evans and T. Abdelnour, Anatomical Data for Analyzing Human Motion. Research Quarterly for Exercise and Sport, 1983. 54(2): p. 169-178.

37. www.controlsandcables.com/assets/Uploads/Bowden1.jpg.

38. Söylemez, E., Makina Teorisi 2 - Makine Dinamigi: Makina Teorisi 2. 2011: Birsen Yayinevi.

39. www.oriental-motor.co.uk.

APPENDIX A

TECHNICAL DRAWINGS

This section contains the technical drawings for prototyping. Before assembly of chassis is shown, there are some elements in detail such as support and parts of triangle. The part called triangle is the connecting section of chassis to the support part. The part called support is the last part of base where re-configuration joint is formed.

Then, fixed link frame is presented. All of following parts are elements attached or joined to fixed link frame. Motor pulley support is attached first and motor pulley is placed inside it. Motor is mounted on the other side of motor pulley support. Other three pulleys represented as pulley 1, pulley 2 and pulley 3 are intermediate pulleys. They are connected to fixed link frame through revolute joints as shown in Figure 48. Finally, moving links of the mechanism are shown in detail.

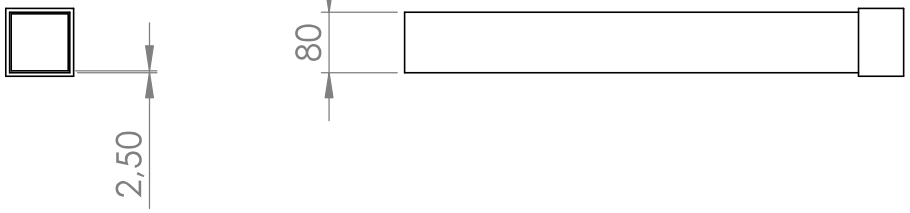

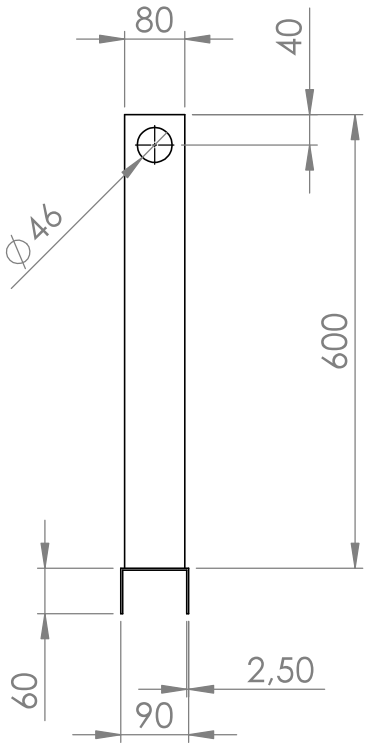

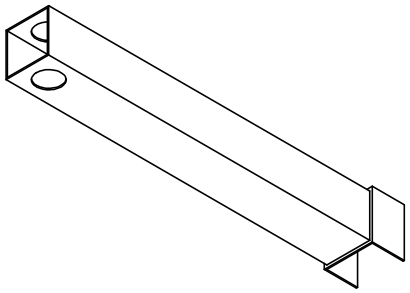

AKSİ BELİRTİLMEDİĞİ SÜRECE: BOYUTLAR MİLİMETREDİR YÜZEY CİLASI: TOLERANSLAR: DOĞRUSAL: AÇISAL:	BİTİRME:	KESKİN KENARLARI PAHLAYİN VE KIRIN	TEKNİK RESMİ ÖLÇEKLENDİRMEYİN	REVİZYON			
	İSİM	İMZA	TARİH			BAŞLIK:	
ÇİZEN							
DENET.							
ONAY.							
ÜRET.							
KALİTE				MALZEME:		RESİM NO. Support	A3
				AĞIRLIK:		ÖLÇEK:1:10	SAYFA 1 / 1

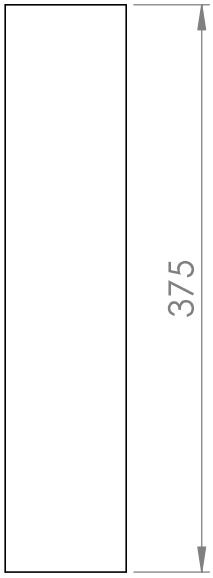

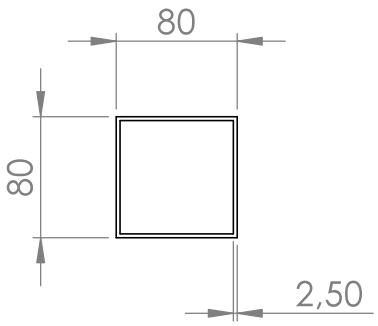

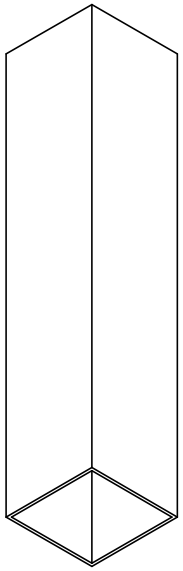

AKSİ BELİRTİLMEDİĞİ SÜRECE: BOYUTLAR MİLİMETREDİR YÜZEY CİLASI: TOLERANSLAR: DOĞRUSAL: AÇISAL:	BİTİRME:	KESKİN KENARLARI PAHLAYIN VE KIRIN	TEKNİK RESMİ ÖLÇEKLENDİRMEYİN / REVİZYON

	İSİM	İMZA	TARİH
ÇİZEN			
DENET.			
ONAY.			
ÜRET.			

BAŞLIK:

KALİTE		MALZEME:	RESİM NO. Triangle1 / A3
AĞIRLIK:		ÖLÇEK:1:5	SAYFA 1 / 1

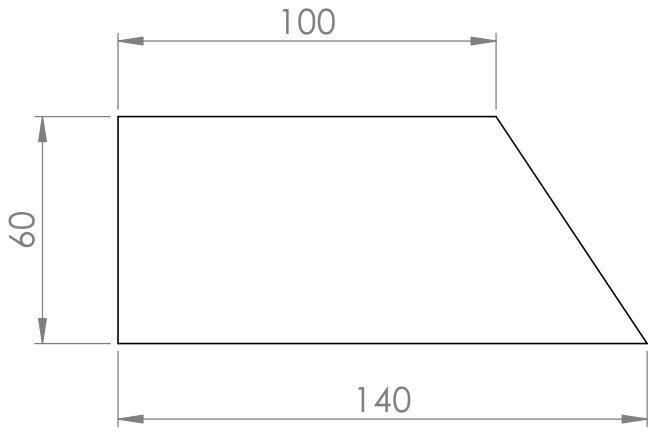

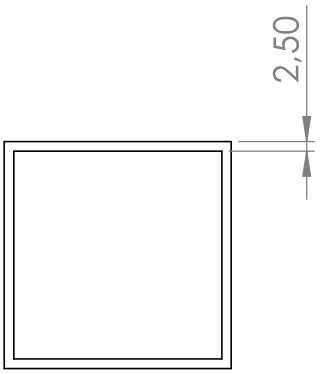

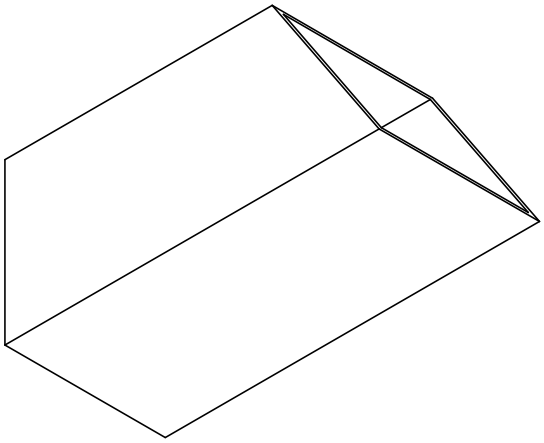

AKSİ BELİRTİLMEDİĞİ SÜRECE: BOYUTLAR MİLİMETREDİR YÜZEY CİLASI: TOLERANSLAR: DOĞRUSAL: AÇISAL:	BİTİRME:	KESKİN KENARLARI PAHLAYİN VE KİRİN	TEKNİK RESMİ ÖLÇEKLENDİRMEYİN	REVİZYON		
	İSİM	İMZA	TARİH			BAŞLIK:
ÇİZEN						
DENET.						
ONAY.						
ÜRET.						
KALİTE				MALZEME:	RESİM NO. Triangle2	A3
				AĞIRLIK:	ÖLÇEK:1:2	SAYFA 1 / 1

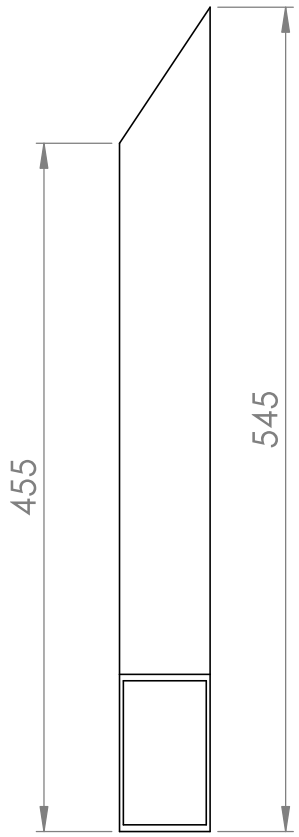

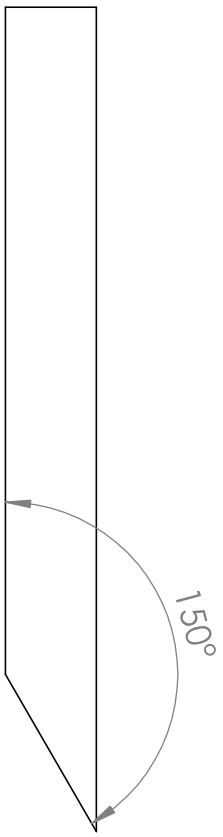

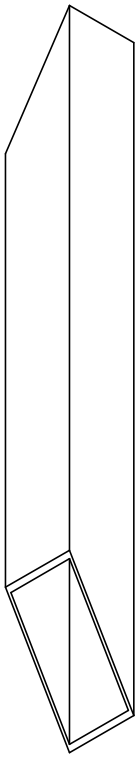

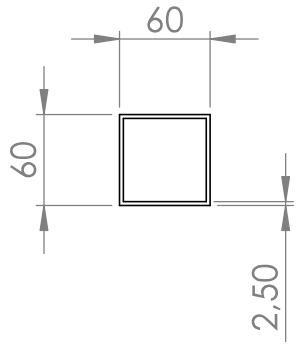

AKSİ BELİRTİLMEDİĞİ SÜRECE: BOYUTLAR MİLİMETREDİR YÜZEY CİLASI: TOLERANSLAR: DOĞRUSAL: AÇISAL:	BİTİRME:	KESKİN KENARLARI PAHLAYIN VE KIRIN	TEKNİK RESMİ ÖLÇEKLENDİRMEYİN / REVİZYON

	İSİM	İMZA	TARİH
ÇİZEN			
DENET.			
ONAY.			
ÜRET.			
KALİTE			

BAŞLIK:

MALZEME:

AĞIRLIK:

RESİM NO.

Triangle3

A3

ÖLÇEK:1:5

SAYFA 1 / 1

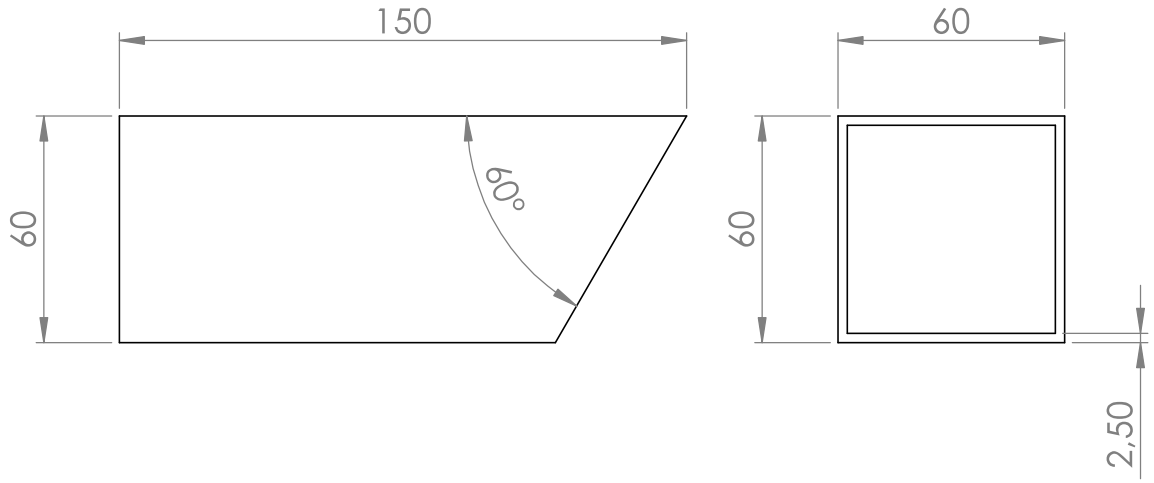

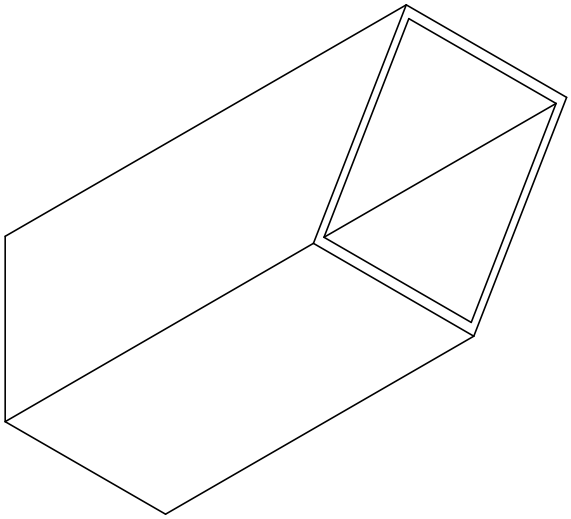

AKSİ BELİRTİLMEDİĞİ SÜRECE: BOYUTLAR MİLİMETREDİR YÜZEY CİLASI: TOLERANSLAR: DOĞRUSAL: AÇISAL:	BİTİRME:	KESKİN KENARLARI PAHLAYİN VE KİRİN	TEKNİK RESMİ ÖLÇEKLENDİRMEYİN	REVİZYON		
	İSİM	İMZA	TARİH			BAŞLIK:
ÇİZEN						
DENET.						
ONAY.						
ÜRET.						
KALİTE				MALZEME:		RESİM NO. A3
						Triangle support
				AĞIRLIK:	ÖLÇEK:1:2	SAYFA 1 / 1

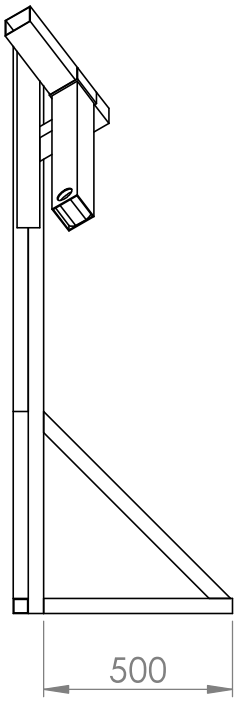

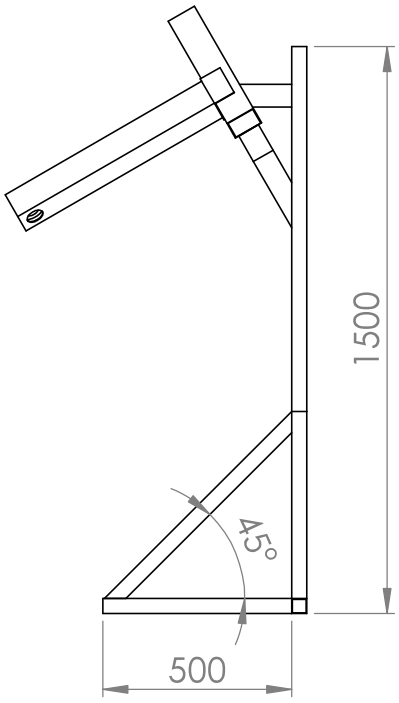

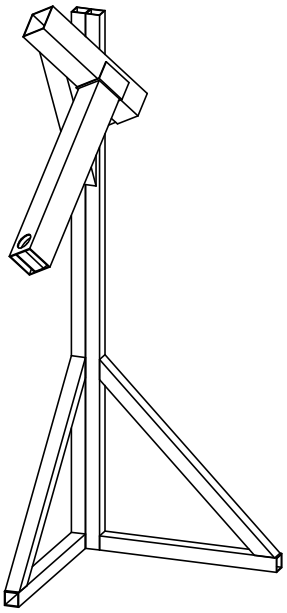

AKSİ BELİRTİLMEDİĞİ SÜRECE: BOYUTLAR MİLİMETREDİR YÜZEY CİLASI: TOLERANSLAR: DOĞRUSAL: AÇISAL:	BİTİRME:	KESKİN KENARLARI PAHLAYIN VE KIRIN	TEKNİK RESMİ ÖLÇEKLENDİRMEYİN	REVİZYON		

	İSİM	İMZA	TARİH			
ÇİZEN						
DENET.						
ONAY.						
ÜRET.						
KALİTE				MALZEME:	RESİM NO.	A3
					Chasis	
				AĞIRLIK:	ÖLÇEK:1:20	SAYFA 1 / 1

BAŞLIK:

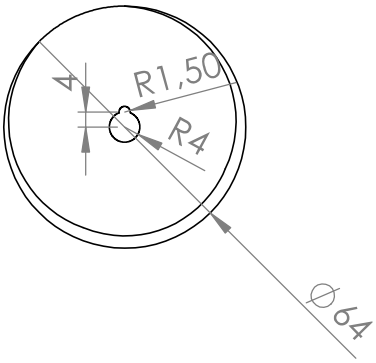

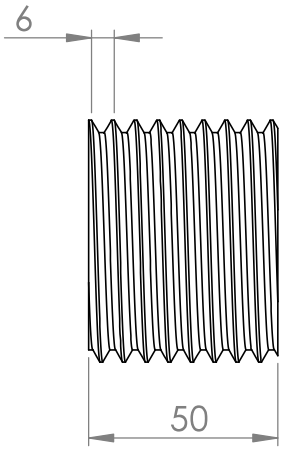

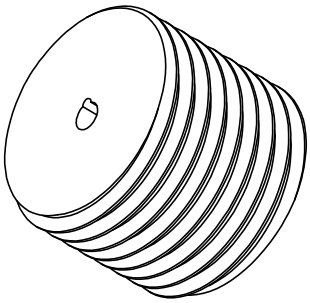

AKSİ BELİRTİLMEDİĞİ SÜRECE: BOYUTLAR MİLİMETREDİR YÜZEY CİLASI: TOLERANSLAR: DOĞRUSAL: AÇISAL:	BİTİRME:		KESKİN KENARLARI PAHLAYIN VE KIRIN		TEKNİK RESMİ ÖLÇEKLENDİRMEYİN	REVİZYON	
	İSİM	İMZA	TARİH			BAŞLIK:	
ÇİZEN							
DENET.							
ONAY.							
ÜRET.							
KALİTE				MALZEME:		RESİM NO.	A3
						Motor Pulley	
				AĞIRLIK:		ÖLÇEK:1:2	SAYFA 1 / 1

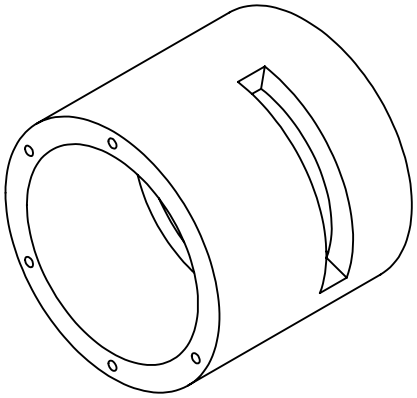

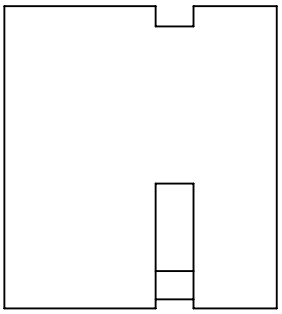

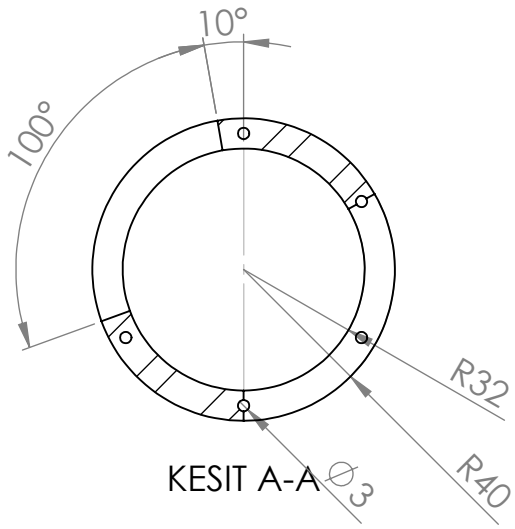

KESIT A-A

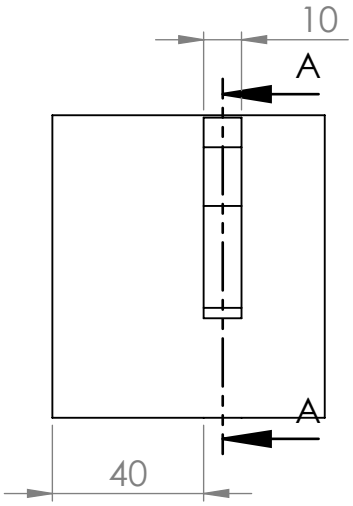

AKSİ BELİRTİLMEDİĞİ SÜRECE: BOYUTLAR MİLİMETREDİR YÜZEY CİLASI: TOLERANSLAR: DOĞRUSAL: AÇISAL:	BİTİRME:	KESKİN KENARLARI PAHLAYIN VE KIRIN	TEKNİK RESMİ ÖLÇEKLENDİRMEYİN	REVİZYON		

	İSİM	İMZA	TARİH			
ÇİZEN						
DENET.						
ONAY.						
ÜRET.						
KALİTE				MALZEME:	RESİM NO.	A3
				AĞIRLIK:	ÖLÇEK:1:2	SAYFA 1 / 1

BAŞLIK:

Motor Pulley Support

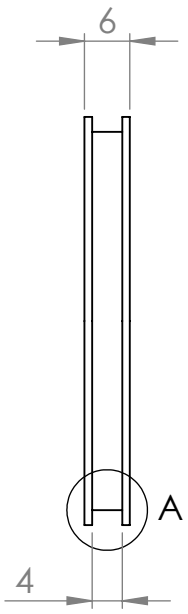

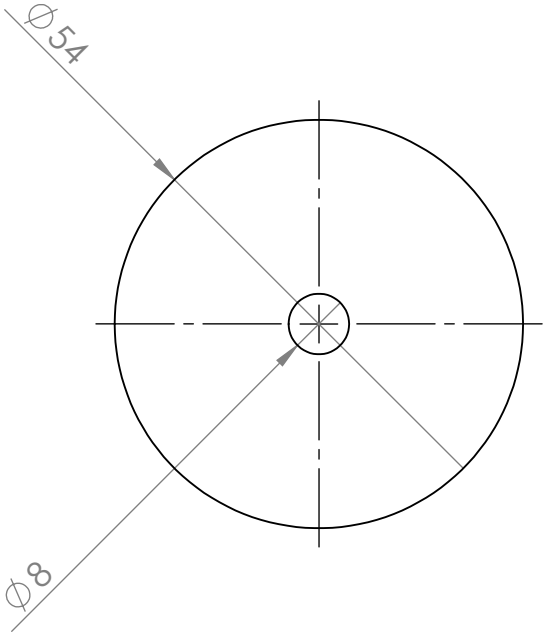

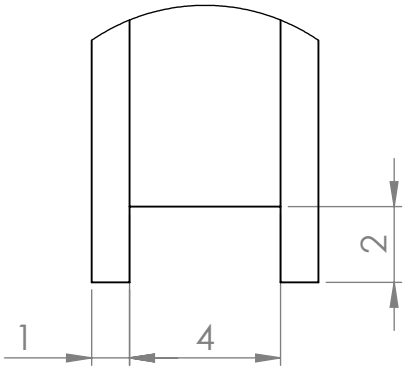

DETAY A
ÖLÇEK 5 : 1

AKSİ BELİRTİLMEDİĞİ SÜRECE: BOYUTLAR MİLİMETREDİR YÜZEY CİLASI: TOLERANSLAR: DOĞRUSAL: AÇISAL:	BİTİRME:	KESKİN KENARLARI PAHLAYIN VE KIRIN	TEKNİK RESMİ ÖLÇEKLENDİRMEYİN	REVİZYON		
	İSİM	İMZA	TARİH		BAŞLIK:	
ÇİZEN						
DENET.						
ONAY.						
ÜRET.						
KALİTE				MALZEME:	RESİM NO. Pulley 1	A3
				AĞIRLIK:	ÖLÇEK:1:1	SAYFA 1 / 1

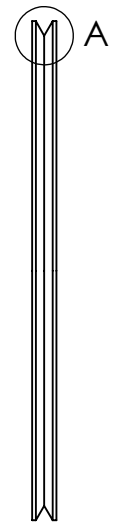

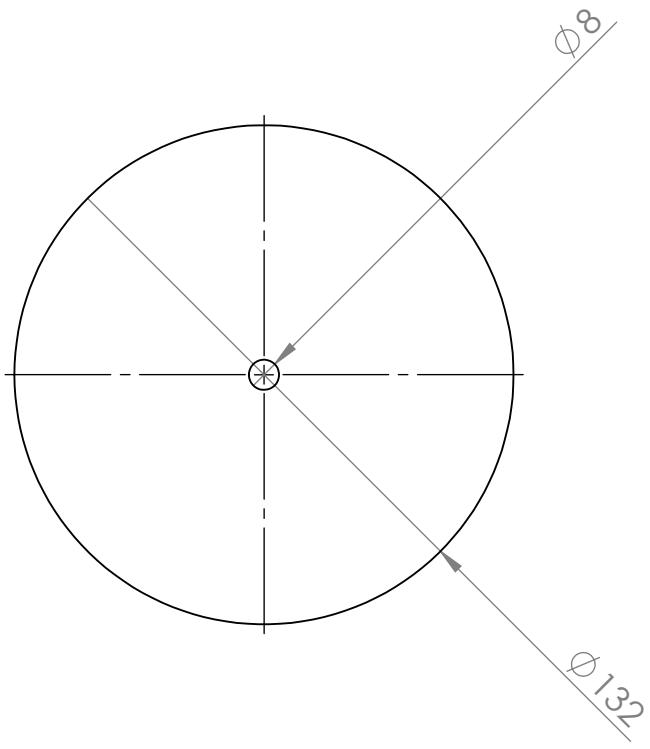

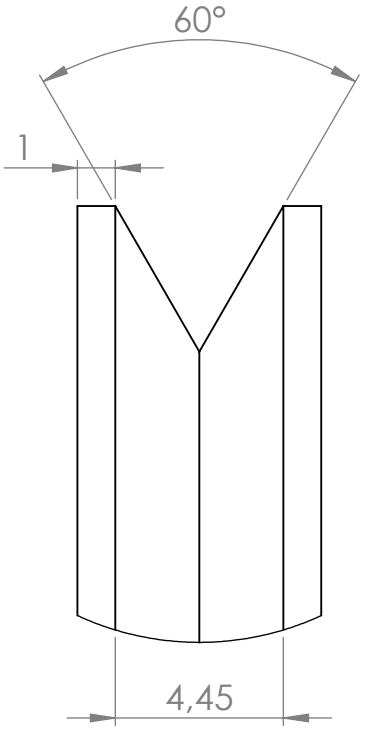

DETAY A
ÖLÇEK 5 : 1

AKSİ BELİRTİLMEDİĞİ SÜRECE: BOYUTLAR MİLİMETREDİR YÜZEY CİLASI: TOLERANSLAR: DOĞRUSAL: AÇISAL:	BİTİRME:	KESKİN KENARLARI PAHLAYIN VE KIRIN	TEKNİK RESMİ ÖLÇEKLENDİRMEYİN	REVİZYON		
	İSİM	İMZA	TARİH		BAŞLIK:	
ÇİZEN						
DENET.						
ONAY.						
ÜRET.						
KALİTE				MALZEME:	RESİM NO. Pulley 2	A3
				AĞIRLIK:	ÖLÇEK:1:2	SAYFA 1 / 1

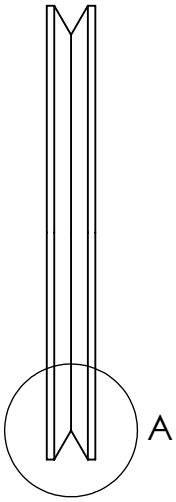

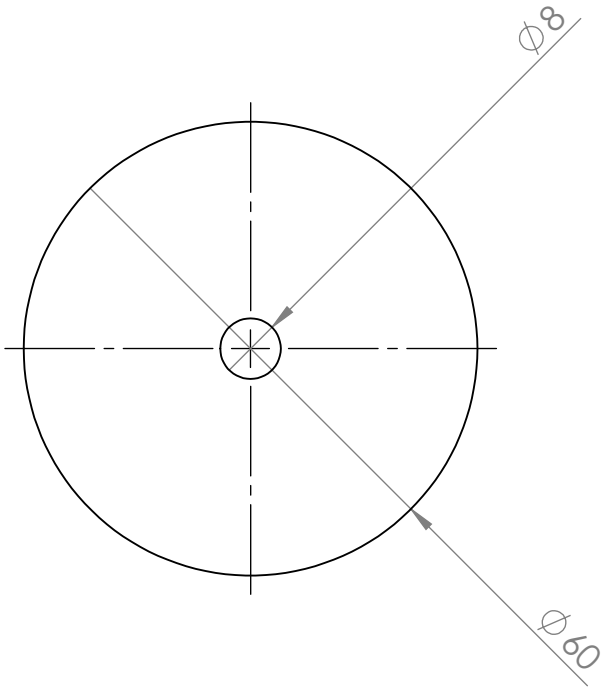

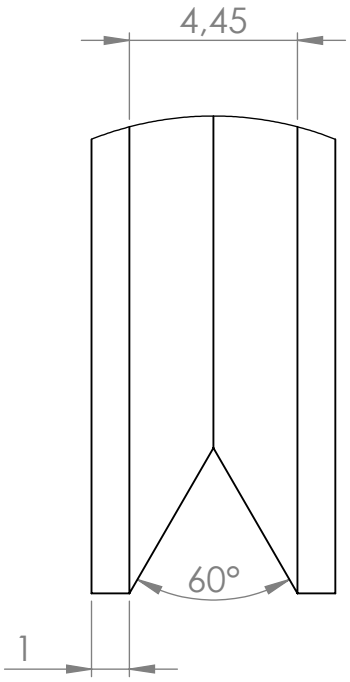

DETAY A
ÖLÇEK 5 : 1

AKSİ BELİRTİLMEDİĞİ SÜRECE: BOYUTLAR MİLİMETREDİR YÜZEY CİLASI: TOLERANSLAR: DOĞRUSAL: AÇISAL:	BİTİRME:	KESKİN KENARLARI PAHLAYIN VE KIRIN	TEKNİK RESMİ ÖLÇEKLENDİRMEYİN / REVİZYON

	İSİM	İMZA	TARİH
ÇİZEN			
DENET.			
ONAY.			
ÜRET.			
KALİTE			

MALZEME:

AĞIRLIK:

BAŞLIK:

RESİM NO.

Pulley 3

A3

ÖLÇEK:1:1

SAYFA 1 / 1

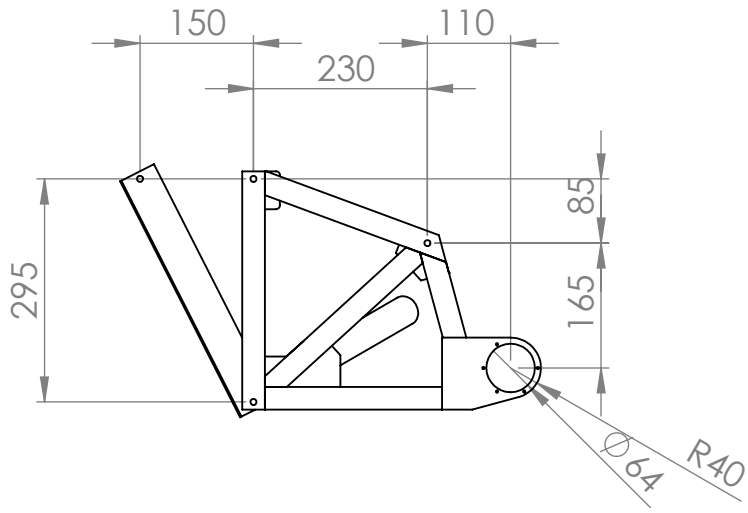

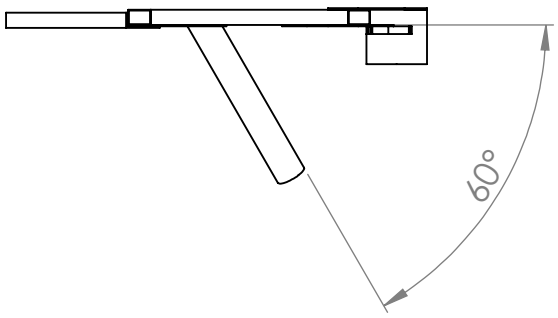

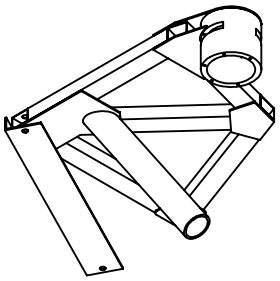

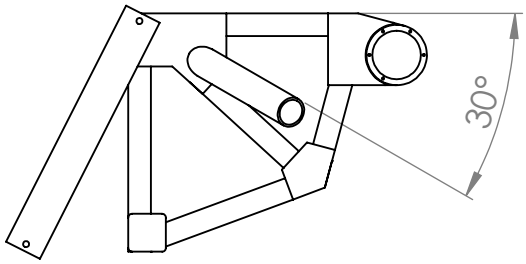

AKSİ BELİRTİLMEDİĞİ SÜRECE: BOYUTLAR MİLİMETREDİR YÜZEY CİLASI: TOLERANSLAR: DOĞRUSAL: AÇISAL:	BİTİRME:	KESKİN KENARLARI PAHLAYIN VE KIRIN	TEKNİK RESMİ ÖLÇEKLENDİRMEYİN / REVİZYON

	İSİM	İMZA	TARİH
ÇİZEN			
DENET.			
ONAY.			
ÜRET.			
KALİTE			

BAŞLIK:

MALZEME:

RESİM NO.

Mechanism Frame

A3

AĞIRLIK:

ÖLÇEK:1:10

SAYFA 1 / 1

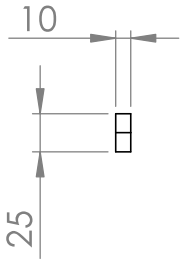

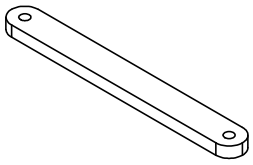

AKSİ BELİRTİLMEDİĞİ SÜRECE: BOYUTLAR MİLİMETREDİR YÜZEY CİLASI: TOLERANSLAR: DOĞRUSAL: AÇISAL:	BİTİRME:	KESKİN KENARLARI PAHLAYIN VE KIRIN	TEKNİK RESMİ ÖLÇEKLENDİRMEYİN / REVİZYON

	İSİM	İMZA	TARİH
ÇİZEN			
DENET.			
ONAY.			
ÜRET.			

BAŞLIK:

KALİTE		MALZEME:	RESİM NO. crank / A3
AĞIRLIK:		ÖLÇEK:1:5	SAYFA 1 / 1

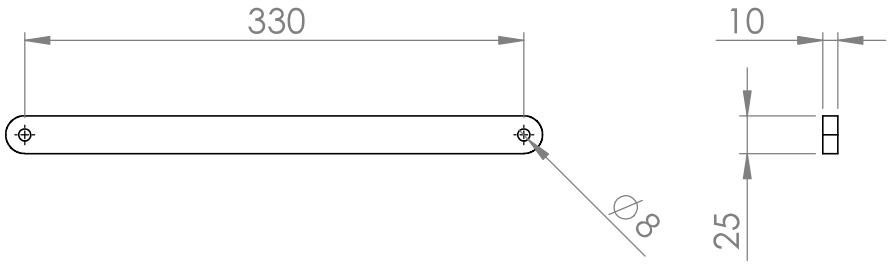

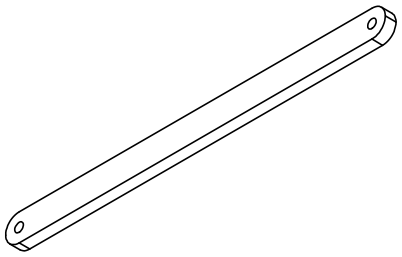

AKSİ BELİRTİLMEDİĞİ SÜRECE: BOYUTLAR MİLİMETREDİR YÜZEY CİLASI: TOLERANSLAR: DOĞRUSAL: AÇISAL:	BİTİRME:	KESKİN KENARLARI PAHLAYIN VE KIRIN	TEKNİK RESMİ ÖLÇEKLENDİRMEYİN / REVİZYON

	İSİM	İMZA	TARİH
ÇİZEN			
DENET.			
ONAY.			
ÜRET.			

BAŞLIK:

KALİTE		MALZEME:	RESİM NO. Rocker / A3
AĞIRLIK:		ÖLÇEK:1:5	SAYFA 1 / 1

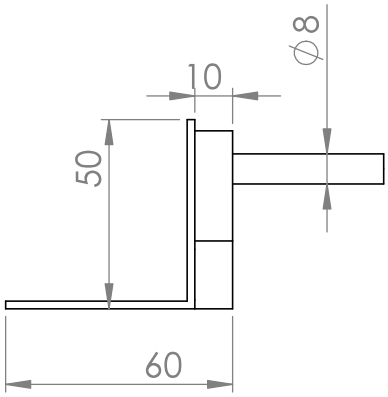

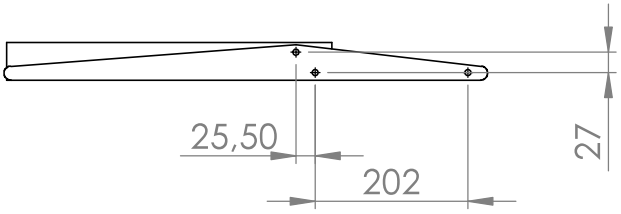

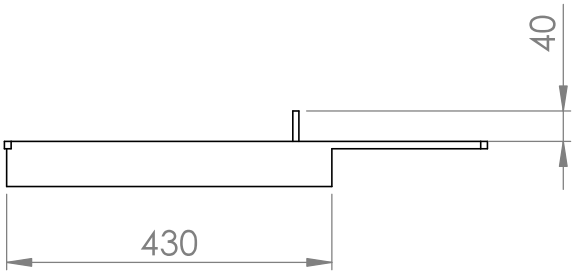

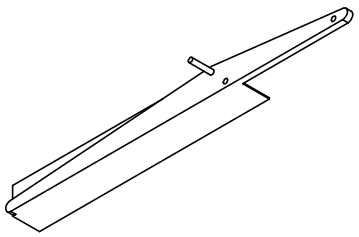

AKSİ BELİRTİLMEDİĞİ SÜRECE: BOYUTLAR MİLİMETREDİR YÜZEY CİLASI: TOLERANSLAR: DOĞRUSAL: AÇISAL:	BİTİRME:	KESKİN KENARLARI PAHLAYIN VE KIRIN	TEKNİK RESMİ ÖLÇEKLENDİRMEYİN / REVİZYON

	İSİM	İMZA	TARİH
ÇİZEN			
DENET.			
ONAY.			
ÜRET.			

BAŞLIK:

KALİTE		MALZEME:	RESİM NO. coupler_extended A3
AĞIRLIK:		ÖLÇEK:1:10	SAYFA 1 / 1